Summer 2007

Late Holocene Uplift of the Chihshang segment of the Longitudinal Valley Fault at Fuli, Eastern Taiwan

Brian Thomas Gray
Central Washington University

LATE HOLOCENE UPLIFT OF THE CHIHSHANG SEGMENT OF THE LONGITUDINAL VALLEY FAULT AT FULI, EASTERN TAIWAN

A Thesis

Presented to

The Graduate Faculty

Central Washington University

In Partial Fulfillment

of the Requirements for the Degree

Master of Science

Geology

---

by

Brian Thomas Gray

August 2007

CENTRAL WASHINGTON UNIVERSITY

Graduate Studies

We hereby approve the thesis of

Brian Thomas Gray

Candidate for the degree of Master of Science

APPROVED FOR THE GRADUATE FACULTY

Date	Dr. Charles M. Rubin, Committee Chair
Date	Dr. Lisa Ely
Date	Dr. Beth Pratt-Sitaula
Date	Associate Vice President of Graduate Studies

ABSTRACT

LATE HOLOCENE UPLIFT OF THE CHIHSHANG SEGMENT OF THE LONGITUDINAL VALLEY FAULT AT FULI, EASTERN TAIWAN

by

Brian Thomas Gray

August 2007

Uplifted Holocene strath terraces of the Bieh River drainage, eastern Taiwan, were analyzed in order to determine millennial-scale uplift and horizontal shortening rates of the Longitudinal Valley fault. Detrital charcoal fragments collected from three terraces within the Bieh River drainage yield ages between 1395 and 555 cal. yr B.P, suggesting an average uplift rate of 11.3 ± 3.6 mm yr^{-1} for the last 1400 cal. yr B.P. The average horizontal shortening rate of 19.7 ± 9.5 mm yr^{-1} was within error of present-day conventional geodetic measurements, but near the lower limit of the geodetic measurements. This suggests that present-day horizontal shortening may not reflect the millennial-scale nature of horizontal shortening across the Chihshang segment of the Longitudinal Valley fault. Based on the longitudinal profile and several distinct regional geomorphic features, the Bieh River may be experiencing differential deformation outside of the main Longitudinal Valley fault zone, possibly on the Yungfong fault, or unrecognized structures within the Lich Mélange.

ACKNOWLEDGEMENTS

First and foremost, I would like to thank my thesis advisor, Dr. Charles Rubin, for giving me the opportunity to study abroad and for continued support for the last few years. I would also like to thank my committee members, Dr. Lisa Ely, Dr. Beth Pratt-Sitaula, and Dr Rubin, for their help in improving this manuscript. This project would not have been possible without the support of my colleagues from National Taiwan University, namely Dr.'s Wen-Shan and Yue-Gau Chen. Many thanks to them and their students, especially Yung-Chuan Chen, I-Chin Yen, Yao-Kao Chu, and Chih-Chang Barry Yang, for the overwhelming amount of logistical support, labor, and hospitality they provided during my visits Taiwan. Thanks to Dr. Bruce Shyu for proposing this study. Thanks to Yun-Ruey Chuang for our many conversations of Taiwan tectonics. Thanks to Ana Aguiar for her support during the last two years, and for her wealth of Word and Excel wisdom she lent whenever asked. I would also like to thank my parents, Ron and Karol Gray, for supporting my endeavors these last few years.

This project was partially funded by National Science Foundation (NSF) EAR #020844 grant, a Geological Society of America graduate student research grant, a 2005 National Science Foundation Summer Institute in Taiwan graduate fellowship, and the Central Geologic Survey of Taiwan

TABLE OF CONTENTS

TABLE OF FIGURES

CHAPTER I

INTRODUCTION

Objectives

The Island of Taiwan, located in the western Pacific Ocean approximately 130 km east of mainland China, occupies one of the most dynamic tectonic settings in the world (Figure 1). Within the past century, Taiwan has experienced nine strong to major earthquakes M_w 6.5 or greater with an associated 6000 deaths (Bonilla, 1999), most notably the 1999 Chi-Chi earthquake which resulted in over 2300 deaths (Liao *et al.*, 2003) and an estimated $12 billion in damage (Chen, 2001). Taiwan is a relatively small island with a total mainland land area of less than 33,000 km^2, with a population of almost 23 million people (United States Central Intelligence Agency, 2007), making it one the most densely populated nations in the world. With a dense population and rapidly developing economy and infrastructure, regional earthquakes pose a significant hazard to the national infrastructure and economy. Given the high likelihood of future damaging earthquakes in Taiwan, it is important that the processes of faulting, seismic rupture, and interseismic deformation be well understood to help mitigate the effects of future large earthquakes.

Currently, little is known about the millennial-scale slip behavior of the Longitudinal Valley fault (Figure 1) as most slip-rate studies have relied on geodetic or late Holocene paleoseismic data. For example, is the modern slip rate of the Longitudinal Valley fault representative of millennial-scale slip or are long-term slip rates slower than current geodetic and geologic data suggest? Documenting millennial-scale geologic slip

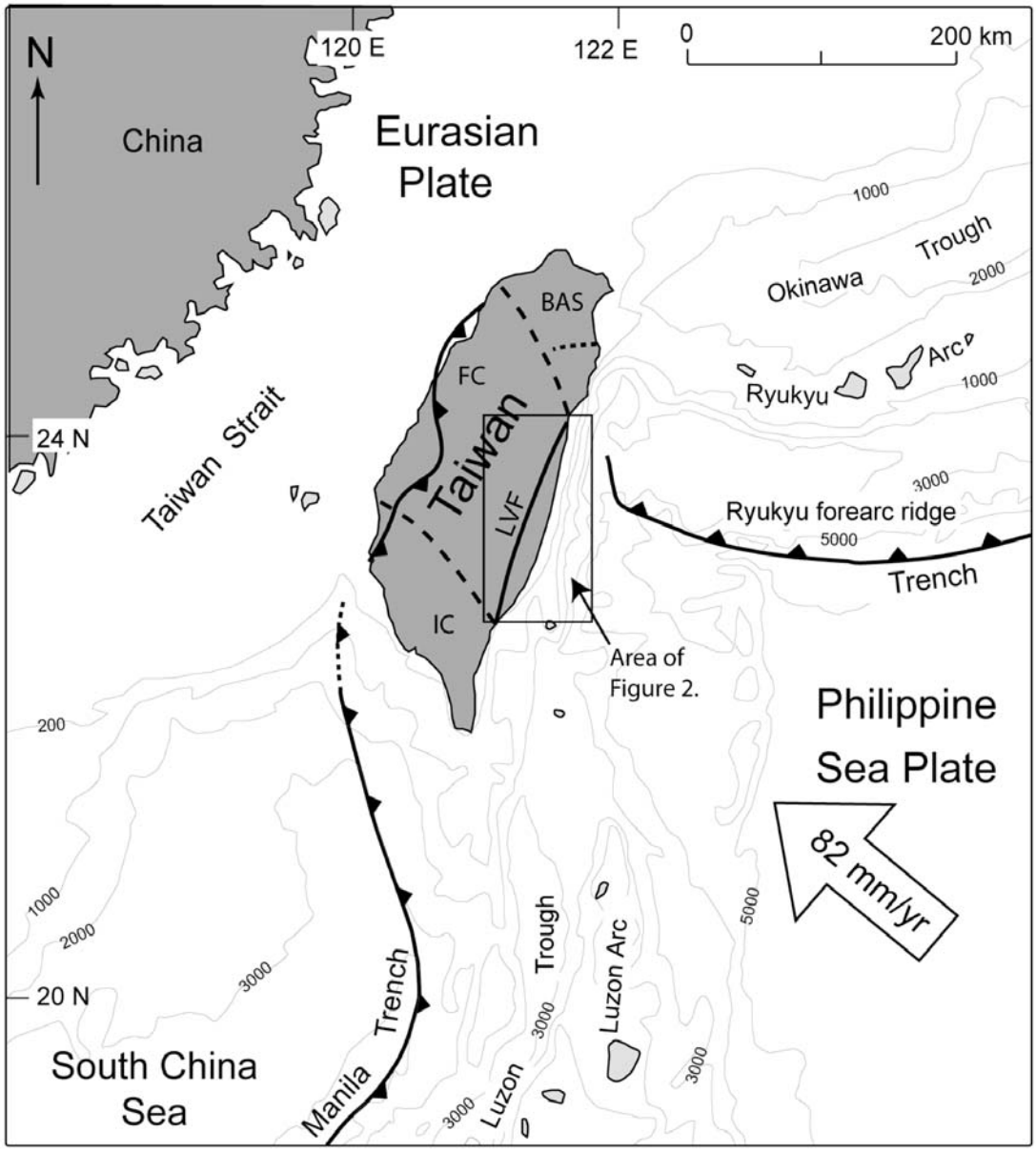

Figure 1. Tectonic map showing the complex tectonic nature of the Taiwan plate margin. Subduction of the Eurasian plate oceanic crust occurs south of Taiwan whereas the Philippine Sea plate is subducting beneath the Eurasian plate east of northern Taiwan. The three major tectonic regimes of Taiwan are shown as initial collision (IC) in the south, full collision (FC) in central Taiwan, and back-arc spreading and orogenic collapse (BAS) in the north. GPS vectors from Yu et al. (1997). Modified from Suppe (1984).
.

rates will help to determine whether current geodetic measurements reflect the true millennial-scale slip rates of the Longitudinal Valley fault. The objective of this study is to characterize the millennial-scale nature of faulting along the Chihshang segment of the Longitudinal Valley fault (Figure 2). Specifically, the study goals are to: (1) document uplift and horizontal shortening rates of the Chihshang segment of the Longitudinal Valley fault by measuring and dating uplifted strath terraces of the Bieh River near Fuli (Figure 2); (2) compare present-day annual and decadal-scale horizontal shortening rates with rates obtained from the Bieh River strath terraces; (3) use the geomorphology of the Bieh River to document Holocene faulting and deformation in the Bieh River/Fuli area.

Tectonic Setting

The island of Taiwan rests on the eastern margin of the stable Eurasian plate, a product of collision of the Phillipine Sea and Eurasian plates (Figure 1). The active collisional nature of the Eurasian\Phillipine Sea plate boundary produced the Taiwan orogen over the past few million years (Chi *et al.*, 1981). Using 1990-1995 global positioning system (GPS) data from the Taiwan GPS network, Yu *et al.* (1997) show the Philippine Sea plate is converging at a rate of ~82 mm/yr with respect to the stable Eurasian plate, oblique to Taiwan's eastern coastline (Figure 1). Geodetic shortening rates slow progressively to the northwest (Yu *et al.*, 1997) as Philippine Sea plate motion is transferred to north-south-trending thrust faults beneath Taiwan, and the oblique reverse Longitudinal Valley fault bounding the western margin of Taiwan's Coastal Range (Figure 1). Oblique convergence of the Phillipine Sea plate in the Taiwan region results in a 94 mm yr^{-1} north to south migration of the suture zone (Suppe, 1984).

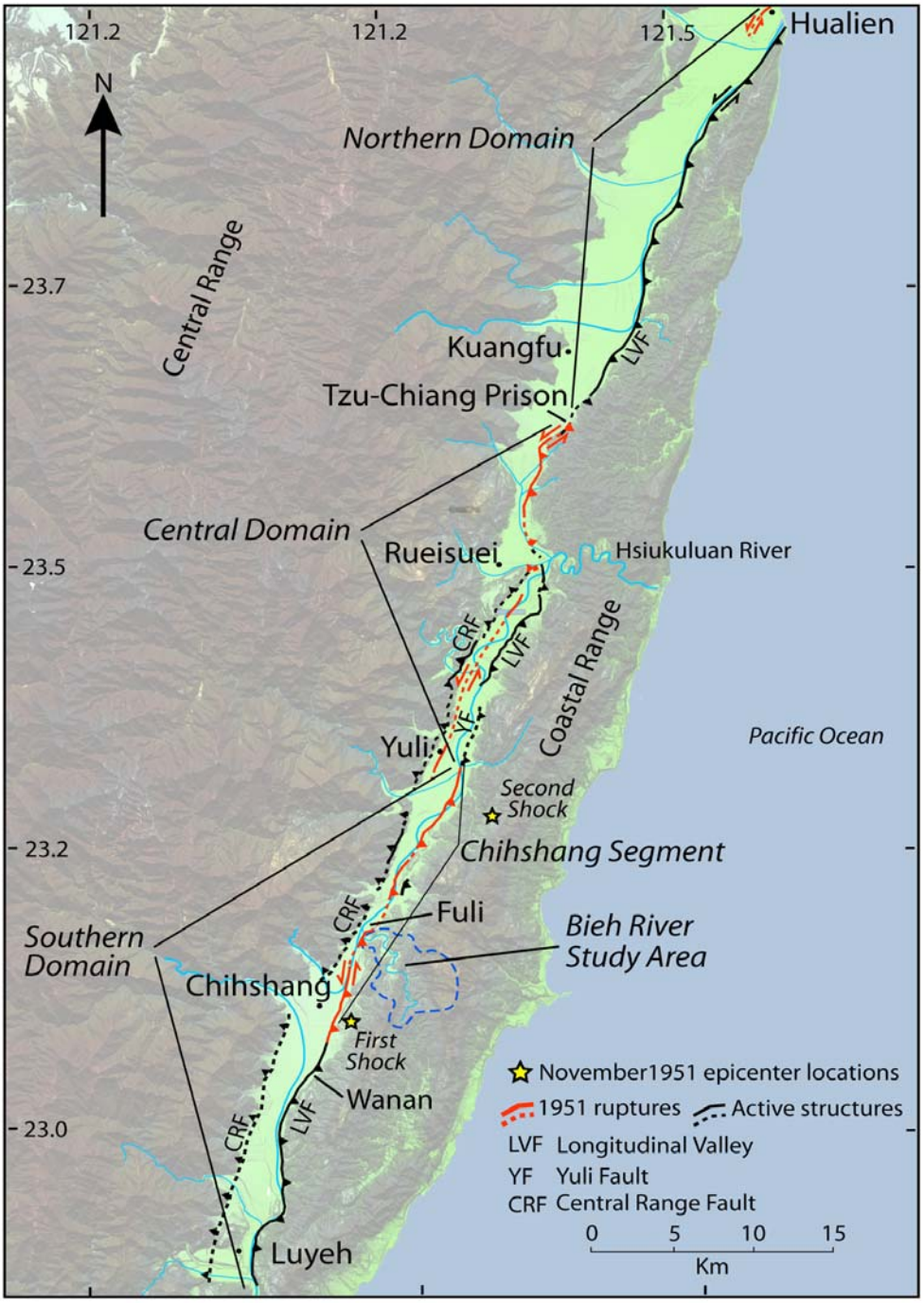

Figure 2. Neotectonic map of the Longitudinal Valley showing major active faults (black) and fault segments from the October and November, 1951 earthquakes (red). The 45 km^2 study area is located southeast of the town of Fuli in the Southern Domain. Geology modified from Shyu *et al*. (2007).

Migration of the suture zone results in incipient collision in the south, full collision in central Taiwan, and orogenic collapse in northern Taiwan (Figure1; Shyu *et al.*, 2005b; Suppe, 1984).

The northeast-trending Longitudinal Valley is a 150- km-long valley bounding the eastern margin of Taiwan's Central Range (Figure 2). Valley width ranges between 1 and 7 km and averages 3–4 km, reaching a maximum altitude of over 300 m near Chihshang (Figure 2), where a major drainage divide occurs. The Longitudinal Valley fault accommodates oblique convergence between the Eurasian and Philippine Sea plates; accounting for about 32% of plate-normal shortening and 80% of the plate-parallel motion of the total Philippine Sea-Eurasian plate convergence (Angelier *et al.*, 2000). Bounding the Longitudinal Valley along its western margin, the Longitudinal Valley fault juxtaposes rocks of the Coastal Range with alluvial sediments of the Longitudinal Valley, predominantly derived from the Central Range. Evolution of the arc-continent suture zone likely began 2 Ma or less (Barrier and Angelier, 1986). As Philippine Sea plate motion progressed northwestward, impingement of the Luzon Arc on the Eurasian continental sliver began to form contractional structures, exhuming the accreted rocks of the Luzon Arc-Trough system (Figure 1). Because of the southward propagation of the suture zone, the structures currently located southeast of Taiwan are modern analogs to the initial collisional structures occurring in the present-day northern Longitudinal Valley (Lundberg, *et al.*, 1997).

The evolution of the Longitudinal Valley fault arc-continent suture zone is well documented by the volcanic, volcaniclastic, and sedimentary rocks of the Coastal Range

orogen. The Miocene to early Pliocene Tuluanshan Formation forms the backbone of the Coastal Range and is composed of intermediate igneous and volcaniclastic rocks of the accreted Luzon Arc. Teng *et al.* (1988) describe the Tuluanshan Formation as an assemblage of mainly andesitic lavas and breccias (up to 1000 m thick), with lesser volumes of tuff, intrusive rocks, volcaniclastic rocks, and volcaniclastic rich limestone. (Kangkou Limestone) (Teng *et al.*, 1988; Wang and Chen, 1993). Stratigraphically higher, the Fanshuliao Formation (also known as the Takangkou Formation) consisting of periodic mudstone/sandstone turbidites and mudstones, represents the first major pulse of continental and arc-derived sediment draped over the Tuluanshan Formation as the Luzon Arc was approaching Taiwan's eastern coast. Fanshuliao rocks are likely related to the fore-arc basin based upon the dramatic decrease in stratigraphic thickness from west to east across the arc (Chen and Wang, 1988). The Lichi Mélange, Miocene to Pliocene in age based on fossil assemblages (Chang, 1967; Huang, 1969; Chi *et al.*, 1981; Chen, 1988) is a highly sheared mudstone found along most of the western margin of the southern Coastal Range (Figure 2). The chaotic mudstones of the Lichi Mélange are pervasively sheared and foliated, and contain exotic blocks of ophiolite, sandstone, and Tuluanshan-derived andesite, meters to kilometers in size (Hsu, 1976; Liou, Lan and Earnst, 1977; Page and Suppe, 1981). Key in understanding the nature of faulting along the Chihshang segment of the Longitudinal Valley fault (Figure 2) is the apparent effect Lichi Mélange rocks have on reducing the coupling strength of the fault zone. The Lichi Mélange is highly sheared and poorly indurated in most locales, especially in the Fuli-

Chihshang region, and facilitates creep of the upper few kilometers of the Longitudinal Valley fault.

Structure, Segmentation, and Slip History of the Longitudinal Valley Fault

Using conventional and GPS geodesy (Yu *et al.*, 1997; Yu and Kuo, 2001; Angelier et al., 1997, 2000; Lee *et al.*, 2001, 2003, 2006), rupture history (Hsu, 1962; Chung, 2003; Shyu et al, 2007) and focal mechanisms (Kuochen *et al.*, 2004), the Longitudinal Valley fault can be divided into several tectonic domains, delineated by the unique style of faulting at each locale. Along strike from north to south, both the nature and rate of fault slip vary considerably as a result of differing structural styles, fault orientations, and lithologies (Figure 2). In October and November 1951, numerous fault segments within the northern, central, and southern regimes of the Longitudinal Valley fault (Figure 2) ruptured, resulting in over 80 deaths and damage to thousands of buildings within the valley (Cheng, 1960; Hsu, 1971). The M_w 7.1 October 22 rupture occurred on the Meilun fault north of the city of Hualien (Hsu, 1971) (Figure 2); surface rupture may have propagated into the city itself (Bonilla, 1975). The November 25, 1951 surface rupture involved two separate events 3 minutes apart. The main shock occurred west of the town of Chihshang. Surface rupture occurred along the eastern margin of the Longitudinal Valley, north to the vicinity of Yuli (Figure 2). Rupture along the Yuli fault and the Rueisuei–Kuangfu segment of the Longitudinal Valley fault produced the second shock three minutes later (Figure 2; Hsu, 1962; Shyu *et al.*, 2007). Although rupture of the two segments is reported as contemporaneous, the Yuli and Longitudinal Valley fault

segments are structurally distinct based upon their style of rupture and show little or no overlap along strike (Figure 2).

The northern tectonic domain of the Longitudinal Valley fault extends from the city of Hualien in the north to a region between the villages of Kuangfu and Rueisuei Figure 2; Shyu *et al*., 2005a). The northern domain is characterized by obliquely-convergent left-lateral strike-slip faulting. Recent GPS studies by Yu *et al.* (1997) and Yu and Kuo (2001) show a significant decrease in short-term shortening rates of the northern coastal range block, as well as decreased slip rates along the northern Longitudinal Valley fault. GPS-derived shortening azimuths of the northern Coastal Range (Yu *et al.*, 1997; Yu and Kuo 2001) shift toward the north with respect to shortening azimuths further south, produced by a dominance of sinistral motion along the Longitudinal Valley fault. Northeast-striking reverse faults (Wang and Chen, 1993) accommodate northeast-directed strain within the northern Coastal Range (Yu and Kuo, 2001; Kuochen *et al.*, 2004). Evidence for the dominance of strike-slip motion in the northern domain comes from the October 1951 earthquake where sinistral offsets of 2 m were accompanied by uplift of about 1.2 m (Hsu, 1955; Bonilla, 1975, 1977).

The central domain of the Longitudinal Valley fault extends from the Rueisuei–Kuangfu transition zone in the north, to Yuli in the south (Figure 2), where creep rates of the Longitudinal Valley fault begin to increase (Hsu and Bürgmann, 2006). The central domain of the Longitudinal Valley fault is marked by numerous fault strands as a result of the northern termination of the active Central Range Fault (Shyu *et al.*, 2006) and possible slip partitioning between the Longitudinal Valley and Yuli faults (Figure 2).

Near the town of Yuli, some of the fault-parallel motion of the Philippine Sea plate is perhaps transferred to the strike-slip Yuli fault, rather than occurring as oblique slip on the main Longitudinal Valley fault. Evidence for slip partitioning comes from the surface rupture of the Yuli fault produced during the November 1951 earthquake sequence. During the 1951 earthquake, the Yuli fault likely ruptured from the town of Yuli, north about 20 km, to a preexisting pop-up structure 4 km south of Rueisuei (Shyu *et al.*, 2007) (Figure 2). During the November 1951 surface rupture, the main strand of the Longitudinal Valley fault did not rupture along the Yuli–Hsiukuluan canyon section, except along the 1.5 km overlap of the Yuli and Chihshang faults at the town of Yuli (Figure 2; Hsu, 1962). Earthquake relocation data from Kuochen *et al.* (2004) suggest the Rueisuei–Yuli region is seismically quiet with respect to the southern Longitudinal Valley fault, perhaps due to lower creep rates. The northern ~15 km of the central domain (Rueisuei segment) is characterized by well-defined reverse fault scarps several meters high in places. The Rueisuei segment enters the Coastal Range near Tzu-Chiang Prison approximately 5 km southwest of Kuangfu (Figure 2). During the November 1951 earthquake, vertical displacement along the Rueisuei segment was typically greater than 1 m and more than 2 m locally (Shyu *et al.*, 2007).

The southern domain of the Longitudinal Valley fault, which includes the intensively studied Chihshang segment, extends from Yuli to several kilometers south of the town of Luyeh (Figure 2). The Chihshang segment displays high rates of sinistral-reverse creep facilitated in part by the Lichi Mélange (e.g., Yu and Liu, 1989; Angelier *et al.*, 1997, 2000; Yu and Kuo, 2001; Lee *et al.*, 2001, 2003; Hsu and Bürgmann, 2006),

but also exhibits coseismic rupture (Hsu, 1962; Lee *et al.*, 2006). The Chihshang segment is characterized by a listric geometry, steeply dipping 50°–60° E in the upper ~17 km, shallowing to 45° at depth (Kuochen *et al.*, 2004; Lee *et al.*, 2006; Wu *et al.*, 2006). Creep rates on the main trace of the Chihshang segment are typically on the order of 15−22 mm/yr (Angelier *et al.*, 1997, 2000; Lee and Angelier, 1993; Lee *et al.*, 2001, 2003). Variations in creep rates come from spatial differences of geodetic surveys and different types of measurement apparatus. Natural outcrops of the Chihshang fault are sparse and little is known about fault dip in the aseismic upper few kilometers. During the November 1951 earthquake sequence, rupture occurred first on the Chihshang segment with vertical coseismic displacements typically less than 0.5 m (Bonilla, 1975; Chung, 2003; Shyu *et al.*, 2007). It is unclear whether the disparity in slip magnitudes between the Rueisuei and Chihshang segments is the result of creep-related strain release during the interseismic period prior to the 1951 events. Recent evidence from the 2003 M_w 6.5 Chengkung earthquake shows seismic rupture at depths of 5−25 km (Ching *et al.*, 2004) propagating to the surface as 1−2 cm of coseismic slip, and more than 10 cm of vertical and horizontal postseismic creep occurring up to 120 days after the earthquake (Lee *et al.*, 2006). Based upon the 1951 rupture history, the 2003 Chenkung earthquake, and geodetic surveys, the Chihshang segment of the Longitudinal Valley fault accommodates strain through aseismic creep, coseismic rupture, and postseismic creep. North of the town of Luyeh, northwest-vergent plate motion is likely accommodated on the Longitudinal Valley and Luyeh faults (Figure 2), as suggested by earthquake relocations from the 2006 M_w 6.1 Taitung earthquake (Wu *et al.*, 2006).

Present-Day Uplift and Horizontal Shortening Rates of the Chihshang Segment of the Longitudinal Valley Fault

Documentation of present-day horizontal shortening and uplift rates of the Longitudinal Valley began in the early 1980's with the installation of Academia Sinica's Taiwan GPS network and other conventional geodetic networks located throughout the Longitudinal Valley. As time progressed, more GPS stations, geodetic networks, leveling lines, and creep-monitoring instruments were surveyed, resulting in what is now a relatively clear picture of the present-day horizontal shortening characteristics of the Longitudinal Valley arc-continent suture zone. Horizontal shortening across the suture zone typically increases further to the south, ranging from 7 to 35 mm yr^{-1} with maximums commonly observed in the Fuli–Chihshang region. Uplift rates generally increase toward the south, reaching maximums near the Fuli/Chihshang region.

Fault motion on Chihshang segment of the Longitudinal Valley fault is probably better constrained than at any other location along the Longitudinal Valley. Likely because of it's well-known creeping behavior and rapid shortening, the Chihshang region has been host to a wide array of studies employing leveling (Yu and Liu, 1989), trilateration networks (e.g. Yu *et al.,* 1990; Angelier *et al.,* 1997), GPS arrays (Yu *et al.*, 1997; Yu and Kuo, 2001), creepmeters (Lee *et al.*, 2001, 2003), and infrared synthetic aperture radar (InSAR) monitoring (Hsu and Bürgmann, 2006). These studies suggest: (1) GPS-based horizontal shortening rates (spanning up to tens of kilometers) across the LVF, not including the Central Range, are consistently in the range of 29–33 mm yr^{-1} (Yu *et al.*, 1997; Yu and Kuo 2001); (2) conventional geodetic network-based horizontal shortening

rates measuring deformation on the scale of hundreds of meters to a few kilometers, are typically 20–22 mm yr^{-1}, 10 mm yr^{-1} lower than GPS-derived rates crossing similar fault locations (Angelier *et al.*, 1997; Angelier *et al*., 2000); (3) Coastal Range uplift rates in the Fuli/Chihshang region range from 13–21 mm yr^{-1} (Yu and Liu, 1989; Angelier *et al*., 2000, Hsu and Bürgmann, 2006); and (4) the majority of fault-related deformation is confined to a relatively narrow zone, as narrow as 20 m at Chihshang and up to 120 m wide near Fuli (Yu and Liu, 1989), although InSAR monitoring suggests creep may produce minor deformation several hundred meters from the fault (Hsu and Bürgmann, 2006).

Geomorphic Framework

Numerous studies have attempted to identify relationships between active tectonic processes coupled with climatic variation, and the geomorphic characteristics of bedrock river systems (e.g. Kirby and Whipple, 2001; Kirby, 2004; Merritts *et al.*, 1994; Pazzaglia *et al.* 1998; VanLaningham *et al.*, 2006). Specifically, studies addressed the question; how do bedrock river systems respond to tectonically-induced land-level changes and climatic variation? Or, what can bedrock river morphology tell us about past tectonic and climatic events?

Bedrock rivers, commonly occurring where rivers are actively incising, typically adjust to tectonic or climatic variation through; incision or aggradation, sinuosity variation, and changes in channel width (Whipple, 2004). Typically, river incision occurs as a result of tectonically-induced uplift (e.g., Pazzaglia *et al.*, 1998; Kirby and Whipple, 2001; VanLaningham *et al.*, 2006), relative base level lowering, or a drop in sediment

supply. Conversely, aggradation commonly occurs in rivers with high sediment flux and or base-level rise, often related to climatic variation. Variations in sinuosity are frequently associated with channel gradient or sediment flux variation in which the river channel gradient adjusts to accommodate changes in sediment load and or land level. Sinuosity change is the river's response in maintaining a state of dynamic equilibrium. Physical processes that control variations in channel width are not well understood, but might be a function of upstream drainage area, lithology, sediment flux, and channel gradient.

Rock uplift rates and lithologic variation along the profile of the river appear to strongly influence channel slope and the concavity of the longitudinal profile. Typically, actively and uniformly uplifting rivers show smoothly concave profiles (Pazzaglia *et al.*, 1998), while rivers with differential uplift show variation in profile form with regions of low concavity (Kirby and Whipple, 2001). Whipple (2004) suggests that channels with low concavity reflect channels with an increase in uplift rate downstream. Low concavities also occur in bedrock rivers, where the drainage is undergoing little or no uplift (Pazzaglia *et al.*, 1998). In addition, changes in longitudinal profile form are commonly caused by variation in rock strength (Kirby and Whipple, 2001; VanLaningham *et al.*, 2006).

The spatial distribution and relative abundance of river terraces, both aggradational and strath terraces, can also help interpretations of past tectonic and climatic conditions. Usually, periods of high sediment flux associated with wet eras or postglacial periods, followed by incision, result in the formation of aggradational river

terraces. In contrast, fluvial strath terraces often form during periods of incision and or increased discharge, where lateral channel migration and or incision occur (Burbank and Anderson, 2001). According to Merritts *et al.* (1994), the occurrence of paired and unpaired terraces is a direct indicator of lateral incision. Where lateral incision occurs, unpaired terraces are the commonly found. Where little or no lateral incision occurs, paired terraces are the dominant form. Identifying aggradational or incisional terraces will help document deformation characteristics within the Bieh River drainage.

CHAPTER II

METHODS

Given its proximity to the Chihshang segment of the Longitudinal Valley fault, the Bieh River drainage area (Figure 2) was targeted to study millennial-scale uplift rates of the Longitudinal Valley fault. The Bieh River is one of only two river systems crossing the Longitudinal Valley fault with a well-developed set of fluvial terraces (Figure 2). Assuming that sequential rupture and nearly-continuous creep of the Longitudinal Valley fault produce sequential uplift of the hangingwall (Figure 3), the objective was to determine long-term slip rates of the Chihshang segment of the Longitudinal Valley fault using uplifted terrace surfaces located within the Bieh River drainage basin.

In order to characterize fluvial terraces of the Bieh River drainage, individual fluvial terraces were delineated and coeval fluvial terraces were correlated throughout the basin. The majority of terraces in the Bieh River area have been converted to rice fields, resulting in very planar, easy to define surfaces. Using black and white aerial photographs, fluvial terraces were delineated based on relative position with other existing terrace treads. Since aerial photograph correlation of fluvial terraces was difficult, 5- and 40- m digital elevation models (DEMs) were used to provide direct elevation data with which to correlate and delineate strath surfaces. To supplement several small gaps in the primary high resolution DEM, the 5– m DEM was underlain with a 40– m DEM data set. DEM correlations and delineations of individual and coeval strath surfaces were made based upon terrace tread height above the active channel.

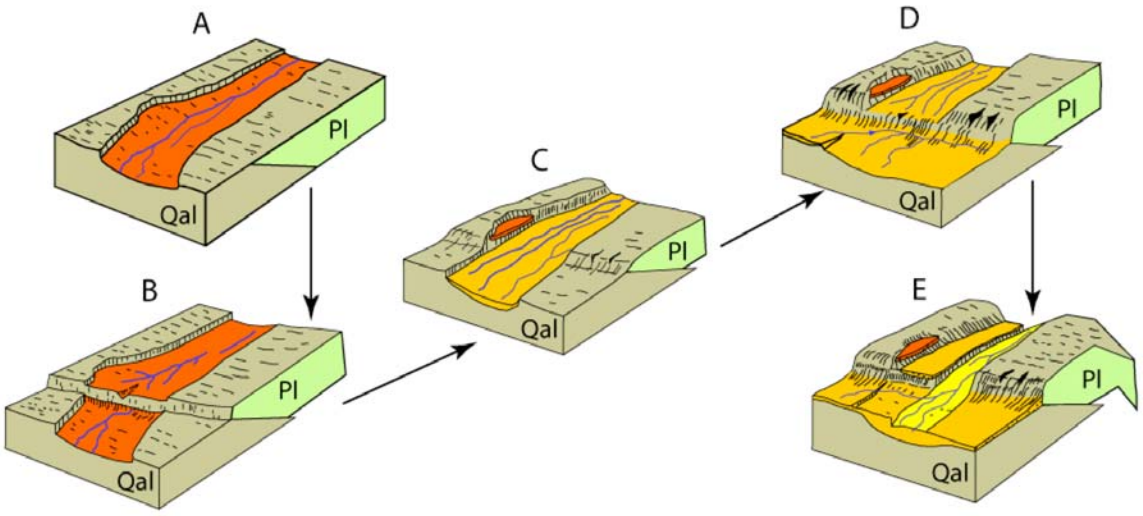

Figure 3. Conceptual model of sequential rupture (resulting from coseismic rupture or aseismic creep), uplift, incision, and strath terrace formation along the main trace of the Longitudinal Valley fault. (A) Initial conditions; prior to rupture, (B) initial rupture results in the formation of a reverse fault scarp, (C) inducing river downcutting, (D) abandonment of the active channel, and (E) strath terrace formation. Multiple occurrences of surface rupture of the Longitudinal Valley fault produce multiple levels of strath terraces. Individual flights of strath surfaces do not necessarily imply an individual rupture. Qal, Quaternary alluvium; Pl, Lichi Mélange.

Because all terrace treads have been modified for farming and the slope of the river channel is not linear, terrace heights vary by up to 15% along the length of the terrace. For this reason, terraces within groups often times had slightly different heights. Terrace height was measured from the center of each terrace, perpendicular to the active channel. Aside from a few small plunge pools, water depth in the Bieh River is typically less than 0.5 m, providing little influence on DEM height measurements. Using aerial photographs, targeted field sites with high elevations above the river, minimal modification, and trackhoe access were identified. With the aid of DEMs and aerial photographs, a Quaternary map was compiled showing fault locations, terrace tread surface locations,

and targeted field sites for shallow excavations to search for ^{14}C samples. Quaternary terraces were mapped directly onto the 5m DEM to produce a detailed and spatially accurate representation of fluvial terraces within the Bieh River drainage. Initial compilation of the Quaternary map began prior to field work and was completed after terraces were mapped and excavated in the field. After the completion of field work, terrace heights and depths to strath were also included with the Quaternary map for comparison.

Field reconnaissance began in late December 2005, locating the specific strath terraces identified with the DEM's and aerial photographs. Sixteen sample locations were selected including natural fluvial terraces exposures, abandoned rice fields, and rice fields between crop rotations. Sample pits were typically excavated to the bedrock strath surface or a maximum depth of 2 m, and typically 3–5 m in length. Each sample pit was mapped, photographed, and sampled, making careful note of sample depths. Although some targeted sites would contain coarse gravels that typically do not preserve detrital charcoal fragments, accelerator mass spectrometry (AMS) ^{14}C was chosen over optically stimulated luminescence because previous optically stimulated luminescence attempts from Taiwan's Coastal Range have been unsuccessful as a result of high denudation rates and lithology (Y. G. Chen, personal comm., 2005). Where possible, detrital charcoal samples or woody fragments were collected from the lower portions of trench exposures to avoid sampling of overbank deposits resulting from post-uplift flood events. Overbank deposits often yield anomalously young ^{14}C results because of lag time between strath

terrace formation and floodplain deposition. Therefore, incision rates calculated from samples collected within overbank deposits represent maximum incision rates.

To aid in the structural interpretation of the Bieh River Drainage, large-scale geologic mapping was performed, focusing along the active river channel, since most of the regional bedrock is concealed by dense vegetation. Compiling map data from this study and those from Wang and Chen (1993) and Chang *et al.* (2001), a geologic map was produced that formed the basis of the Quaternary map.

To better understand basin-wide Holocene deformation and river incision characteristics, a river slope longitudinal profile was constructed in order to document regional deformation characteristics. With the aid of the 5– and 40– m DEMs, a 14– km-long longitudinal profile was produced and then transferred to an image editing program for drafting. Individual points on the profile were recorded with location information. Location information was then used to plot structure and lithology below the profile. Slope was calculated between distinct structural and lithologic boundaries for concavity analysis.

CHAPTER III

OBSERVATIONS AND RESULTS

Structural and Lithologic Observations

The Bieh River drainage basin covers approximately 47.5 km^2 (Figure 2) of the southern Coastal Range, draining rocks of the Fanshuliao, Tuluanshan, and Lichi formations (Plate 1). Three major faults are found within the study area; the Chihshang segment of the Longitudinal Valley fault is located to the west, the central Yungfong fault, and the Tuluanshan fault located in the east (Plate 1). Natural outcrop exposures are generally sparse within the field area and were typically found only within or adjacent to the active Bieh River channel, where nearly all of the geologic observations for this study were documented.

The Lichi Mélange forms the western boundary of the Coastal Range rocks in the Fuli-Bieh River area (Plate 1). Bounded on the west by the Longitudinal Valley fault, highly sheared mudstones of the Lichi Mélange are exposed at several locations within the Bieh River drainage. A small outcrop within several hundred meters of the surface trace of the Longitudinal Valley fault shows Lichi Mélange with shear fabric dipping 60° NW and overlain by unsorted clasts derived from the Central Range. The Lichi Mélange is entirely fault bounded in the Bieh River region. The eastern margin of the Lichi Mélange terminates at the Yungfong fault (Figure 4; Plate 1). Here, the Lichi Mélange is highly sheared, with slickenside scaly foliation planes dipping 45°−70° W (Figure 4). Within 150 m of the Yungfong fault contact, well-developed foliations are present within the mélange mudstone, containing numerous sandstone and siltstone blocks near the

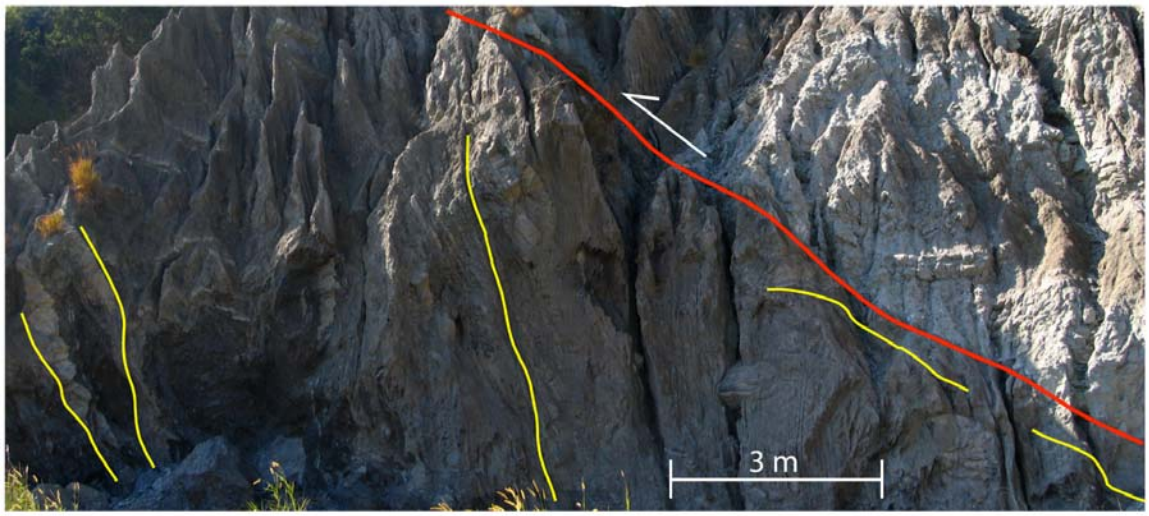

Figure 4. The Lichi Mélange, ~100 m west of the Yungfong fault, looking to the south across the Bieh River. Here, the Lichi Mélange is highly deformed, with one large shear plane (red) parallel to the nearby Yungfong fault and numerous small-scale shears (yellow) oriented sub-parallel to the principle shear plane.

fault zone. East of the Yungfong fault, the Bieh River makes a 90° bend north-northeast (Plate 1). The trace of the Yungfong fault is exposed within 20 m of a main tributary that parallels the Yungfong fault to the south. At its intersection with the Bieh River, the Yungfong fault strikes due north, dipping 42° W (Figure 5). Here, the Yungfong fault zone is marked by a subtle color change and transition in weathering texture from popcorn to non-indurated mudstone. Minor sub-meter-size drag folds of Fanshuliao siltstone beds are also present within the fault zone.

East of the Yungfong fault, the Fanshuliao Formation crops out as an irregularly dipping sequence of mudstone, siltstone and occasional interbedded sandstone (Plate 1). Sandstone interbeds strike north-northeast to northeast and dip 50° northwestward several hundred meters from the Yungfong fault. The dip of sandstone interbeds shallow to 23° NW near the Yungfong fault. Numerous meter-scale east-west-trending faults displacing

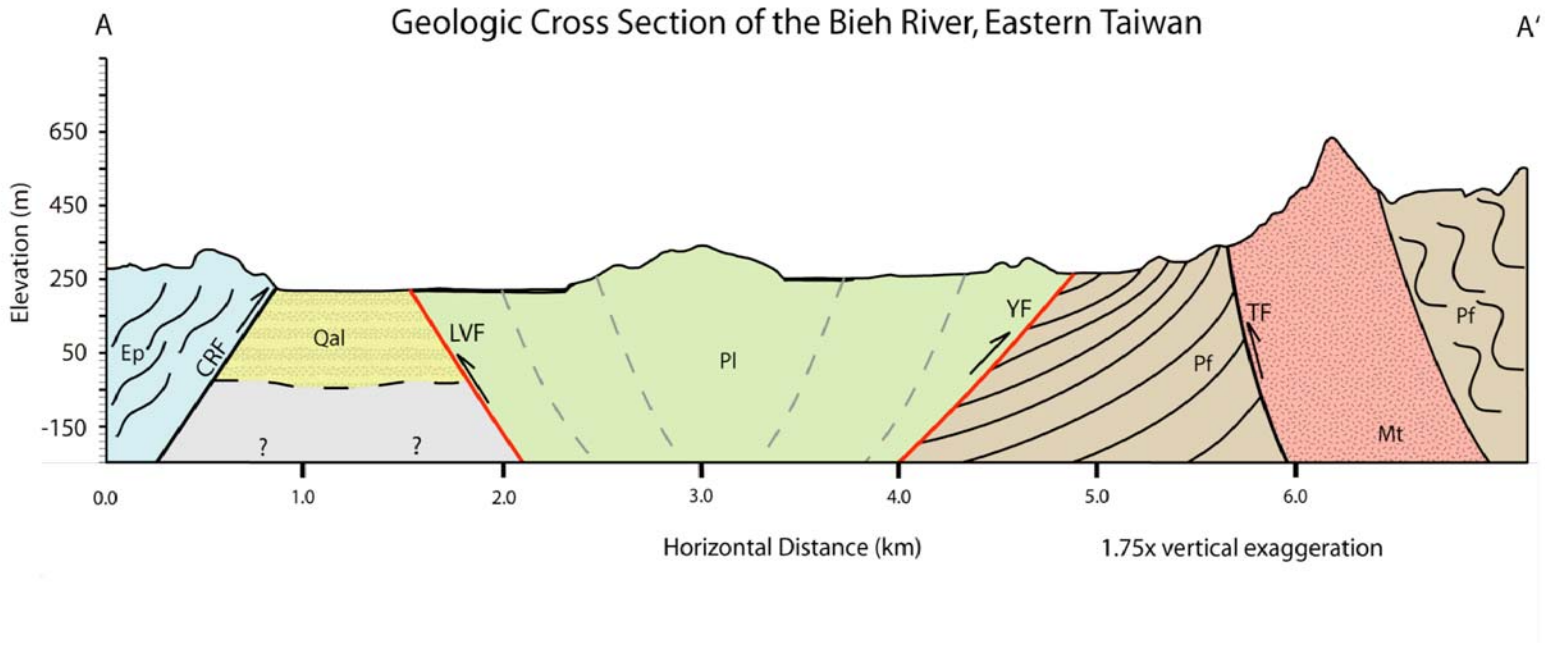

Figure 5. Geologic cross section along A-A' (Plate 1). Note the topographic high within the Lichi formation. Active faults are outlined in red, inactive faults are black. LVF, Longitudinal Valley Fault; CRF, Central Range Fault; YF, Yungfong Fault; TF, Tuluanshan Fault; Ep, Pilushan formation, Pf, Fanshuliao formation, Pl, Lichi Mélange, Mt, Tuluanshan formation. Lichi Mélange shear zones (gray dashed lines) mapped by Chang *et al.* (2001).

sandstone interbeds are present along the dry riverbed. Just over 1 km upstream of the Yungfong fault, lies the eastern faulted contact of the Fanshuliao Formation. Here, the Fanshuliao rocks dip near vertical, overturned in some locations, striking almost due north. The Tuluanshan fault, which forms the contact between the Fanshuliao and Tuluanshan formations, dips near vertical (Figure 5), following the western margin of the prominent north-south trending ridge of Tuluanshan andesitic rocks (Plate 1). The Tuluanshan fault juxtaposes the Tuluanshan volcanic sequence over the stratigraphically younger Fanshuliao Formation. Steep northwest-dipping jointing (~60°) within the Tuluanshan formation is present on the western hillside ~50 m above the fault, while Tuluanshan jointing at the east end of the canyon dips 52° SW (Plate 1). The eastern margin of the Bieh River drainage basin consists of Fanshuliao mudstone and siltstone, which conformably overlies the Tuluanshan sequence on the east side of the Tuluanshan Ridge. Several hundred meters further upstream, Fanshuliao rocks contain numerous small folds and faults.

Spatial Distribution of Bieh River Terraces and River Slope Analysis

Nearly all of the terraces of the Bieh River are located between 2 and 10 km upstream of the confluence with the Hsiukuluan River (Plate 2). Within the first 1.5 km upstream of the Longitudinal Valley fault, terraces are limited to those of the Hsiukuluan River. To the east (upstream), the first major bend in the Bieh River (called Fuli bend in this paper) contains the first set of Bieh River-derived terraces (Plate 2). Here, six sets of Quaternary terraces (Qt2, Qt5, Qt13, Qt13, Qt17, and Qt18) located 4–26 m above the active river channel record seven different periods of river elevation, including the active

channel (Plate 2). The Fuli bend terrace group is the most complete set of terraces in the drainage basin, preserving a record of general northward channel migration, although intermediate terraces are exposed north of the active channel (Plate 1). East of Fuli bend, the majority of river terraces lie along the reach of the Bieh River that is collinear with the Yungfong fault. Spatial distribution analysis of river terraces with respect to distance from the Longitudinal Valley fault shows that 10 of the 27 mapped terraces within the Bieh River drainage lie along the Yungfong reach, 3−3.5 km from the Longitudinal Valley fault (Figure 6A). Terrace elevations along the Yungfong fault typically range from 5 to 17 m above the active river channel, with the exception of Qt 2 located 32.5 m above the channel (Figure 6B; Plate 2). Upstream of the Tuluanshan fault, river terraces are much less abundant and typically low in elevation (Plate 2). Three small terraces, QtI, QtII, and QtIII, are mapped upstream of the contact between the Tuluanshan and Fanshuliao formations. Here, terrace elevations range from 3 to 6 m above the active channel, suggesting only minor amounts of river incision

At the southern end of the Yungfong section, there are two large adjacent terraces located south of the active channel (Qa) that are distinct from other terraces found within the drainage. These terrace treads dip more steeply with respect to the active channel than all other terraces within the drainage (Figure 7), and are exposed 28 and 45 m above the active channel. Along the northern margin of the northern terrace, a natural exposure from a rice field runoff channel displays a terrace exposure of well-sorted coarse gravel, cobble, and coarse sand at least 10 m thick.

A

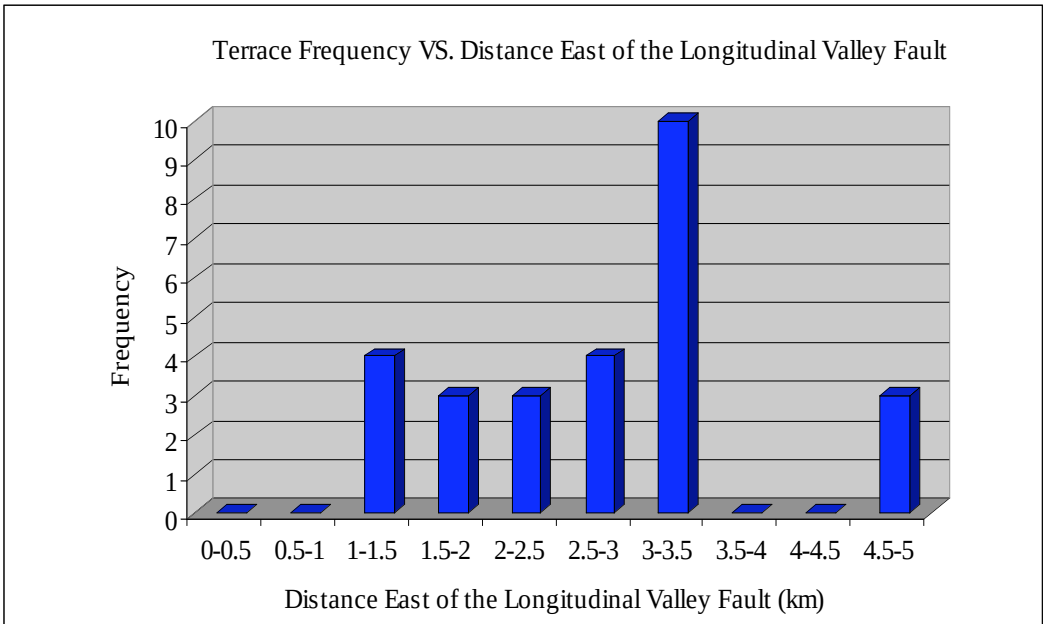

B

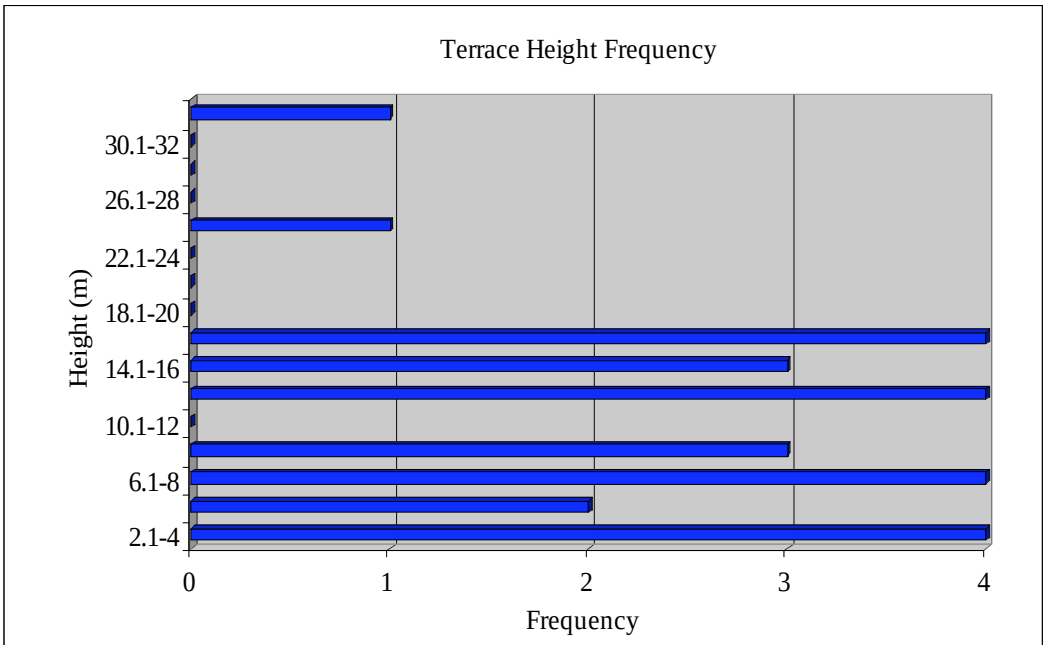

Figure 6. (A) Bieh River terrace frequency versus distance from the Longitudinal Valley fault. Note the abundance of terraces in the 3-3.5 km range, which encompasses the Bieh River reach following the Yungfong fault (Plate 2). (B) Terrace frequency with respect to height above the Bieh River active channel. Only two terraces are preserved above the 18 m level.

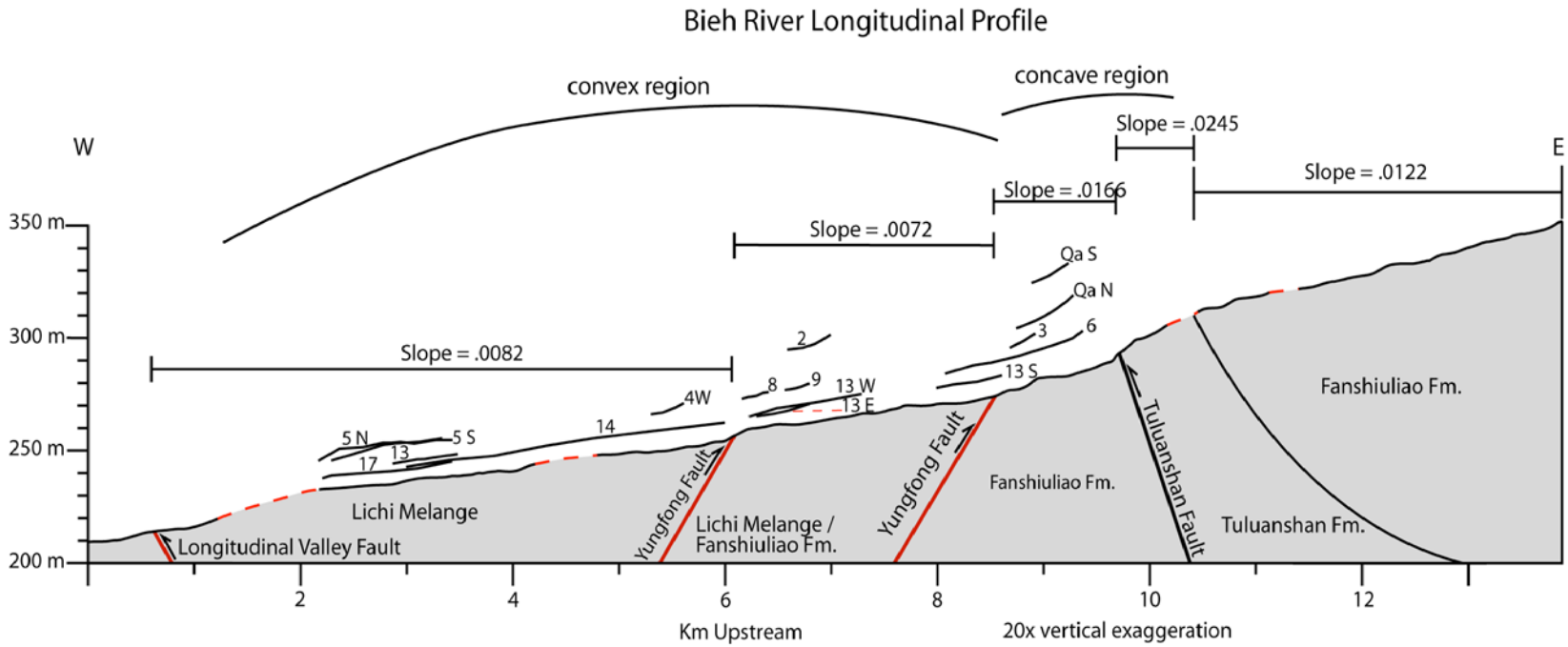

Figure 7. Longitudinal profile of the Bieh River produced from the 5m DEM. Major terrace treads are shown above the profile for comparison of deformation with respect to the active channel. No continuous terrace treads cross the lower trace of the Yungfong fault. The lower reach of the Bieh River, below the upstream Yungfong fault contact, is convex where concavity might be expected for a uniformly uplifting region.

Gradient analysis of the active Bieh River channel and associated terraces yields several insights into the erosional and uplift characteristics of the lower portion of the basin. To the west, river slope variation from the Longitudinal Valley fault to the second crossing of the Yungfong Fault is minimal, changing from 0.0082 along the Longitudinal Valley fault–Yungfong fault section to 0.0072 for the Yungfong section (Figure 7). Crossing the upstream trace of the Yungfong fault to the east, river gradient within the Fanshuliao rocks more than doubles (e.g., 0.0072 to 0.0166), steepening toward the Tuluanshan fault. Channel slope reaches a maximum of 0.245 within the Tuluanshan volcanic rocks, culminating at the Tuluanshan fault (Figure 7). Upstream from Tuluanshan Ridge, channel gradient decreases substantially to 0.0122 as the stream crosses the lithologic boundary into the Fanshuliao formation. Throughout the lower reach of the river from Tuluanshan Ridge (Plate 1) to the Longitudinal Valley fault, slopes of terrace treads typically match those of the active channel (Figure 7), aside from the north and south Qa surfaces (Plate 2).

Geochronology

Seven different river terraces were excavated throughout the Bieh River drainage, some with multiple sample pits. Five of the seven terraces yielded detrital charcoal fragments. Three detrital charcoal samples were collected from Qt6, Qt8, and Qt9 (Plate 2) along the Yungfong reach of the Bieh River. In addition, one fragment of detrital charcoal was collected from the northern Qt5 terrace, and one from the natural strath exposure at QtI (Plate 1). Detrital charcoal fragments were analyzed at the Center for Accelerator Mass Spectrometry at Lawrence Livermore National Laboratory. All three

detrital charcoal fragments collected near the Yungfong fault (Qt6, Qt8, and Qt9) are late Holocene in age (Table 1; Plate 2), ranging from 1365–555 cal. yr B.P. A detrital charcoal fragment collected from Qt5 yielded an age of 5655–5005 cal. yr B.P and a detrital charcoal fragment at QtI yielded an age of 7565–7225 cal. yr B.P. (Table 1; Plate 2).

Typically, terrace deposits consist of coarse sandy gravel and cobble, with minor sand and silt layers that preserve detrital charcoal fragments (Figure 8). All seven trench sites were cultivated for rice farming, resulting in modification of the original terrace tread and addition of clay-rich topsoil. Excavation locations were evenly distributed throughout the drainage, although successful samples were obtained only from the reach bordering the Yungfong fault (Plate 2). Fragments of detrital charcoal at Qt8 and Qt9 were found within coarse gravel (Figure 8), and yielded calendric ages that range between 1365 and 555 cal. yr B.P. (Table 1). A detrital charcoal fragment in Qt6 was collected below a fluvial pea gravel unit likely within a fine overbank sequence (Figure 8). Typically, overbank sediments are considered floodplain deposits, commonly overlying coarse channel deposits near the strath surface. This suggests the Qt6 detrital charcoal fragment was located within a paleo floodplain younger than the strath surface. The fragment of detrital charcoal at the northern Qt 5 surface (Plate 2) was likely recycled detrital charcoal given the calendric age of 5655-5000 cal. yr B.P. and elevation of the terrace. QtI was a naturally exposed strath surface with ~2 m of overlying alluvial cobble, gravel, and sand (Figure 9), yielding an age of 7565–7225 cal. yr B.P. Excavated

Table 1
Radiocarbon Data from Bieh River Sample Locations

Sample	Location	^{14}C age* ±1σ	δ^{13}C†	Calendar Years B.P. (2σ range)‡	Calendar Dates (2σ range)	Sample Height Above Channel (m)	Incision Rate$^{\varphi}$ (mm yr^{-1})	Shortening Rate$^{\eta}$ at 326°
BR6-06-A§	Qt8	1330 ± 40	−25	1365–1225	640–780 A.D.	11.5	8.9 ± 1.4	15.5 ± 4.2
BR8-09-A§	Qt9	545 ± 40	−25	705–555	1300–1440 A.D.	8.1	12.9 ± 2.5	22.5 ± 6.3
BR16-11-A§	Qt6	1355 ± 35	−25	1395–1235	610–770 A.D.	15.8	12.1 ± 2.1	21.1 ± 5.8
BR12-01-B§	Qt5	4610 ± 100	−25	5655–5005	3650–3000 B.C.	10.0	1.9 ± 0.3	3.3 ± 0.9
BR17-01§	QtI	6450 ± 100	−25	7565–7225	5560–5220 B.C.	6.5	0.9 ± 0.1	1.6 ± 0.4

§ Samples processed and accelerator mass spectrometry ^{14}C measurement performed at the Center for Accelerator Mass Spectrometry at Lawrence Livermore National Laboratory.

* The quoted age is in radiocarbon years using the Libby half life of 5568 years; relative to A.D. 1950.

† δ^{13}C values are the assumed values according to Stuiver and Polach (1977) when given without decimal places.

‡ Radiocarbon ages calibrated with OxCal v. 3.10 calibration software (C. Bronk Ramsey, 2005)

φ Error calculation uses 2σ cal. yr B.P. age range and assumes a 15% variability in elevation measurement from DEM.

η Error calculation assumes propagation of error from incision rate calculation, ± 3° for the GPS shortening vector, and ± 5° for the fault dip angle.

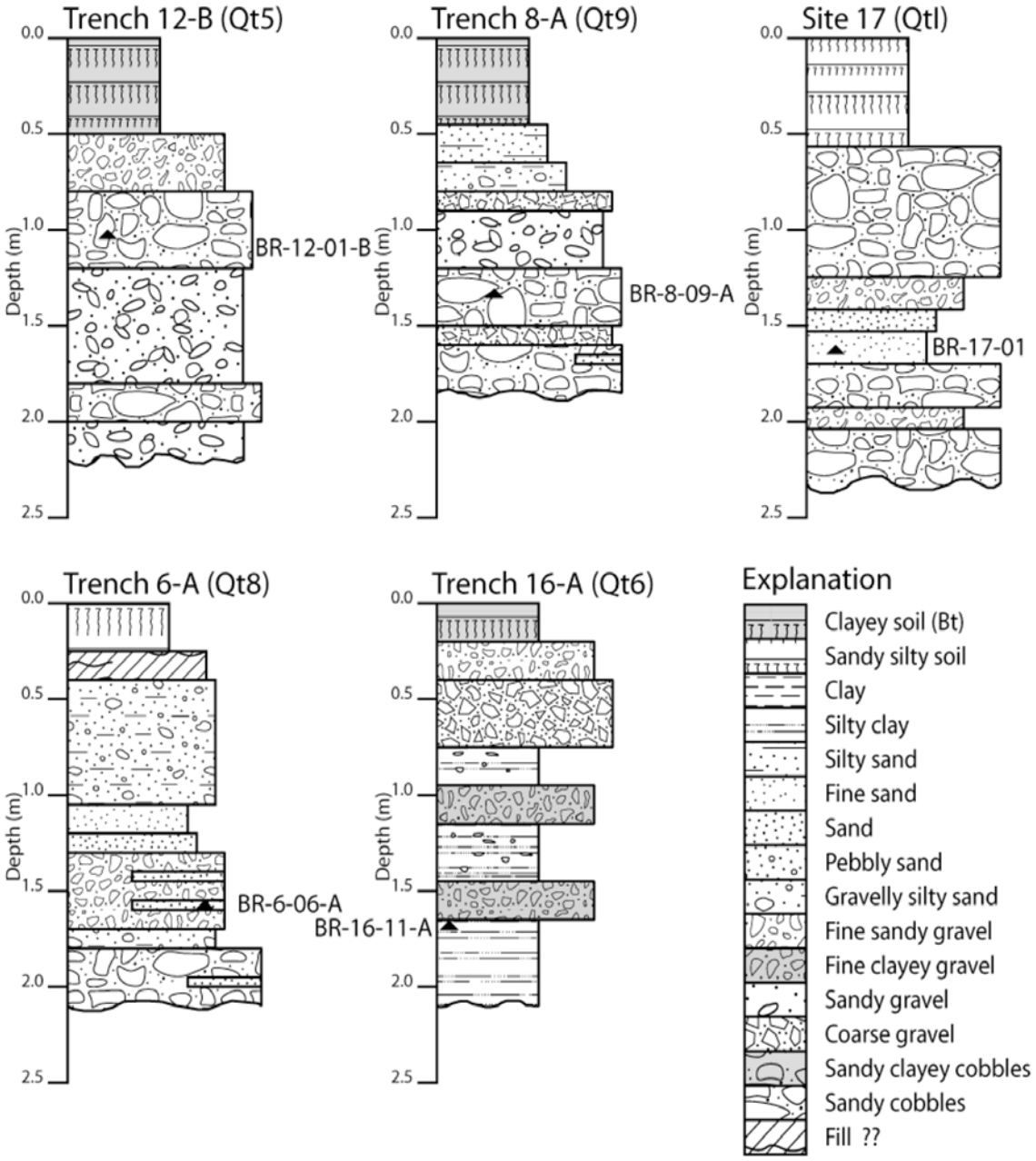

Figure 8. Terrace stratigraphy of the Beih River showing detrital charcoal sample locations. All trench sites contained fine grained soil in the upper 30-50 cm from agricultural modification. Most trench-wall exposures contained abundant coarse gravel and boulders.

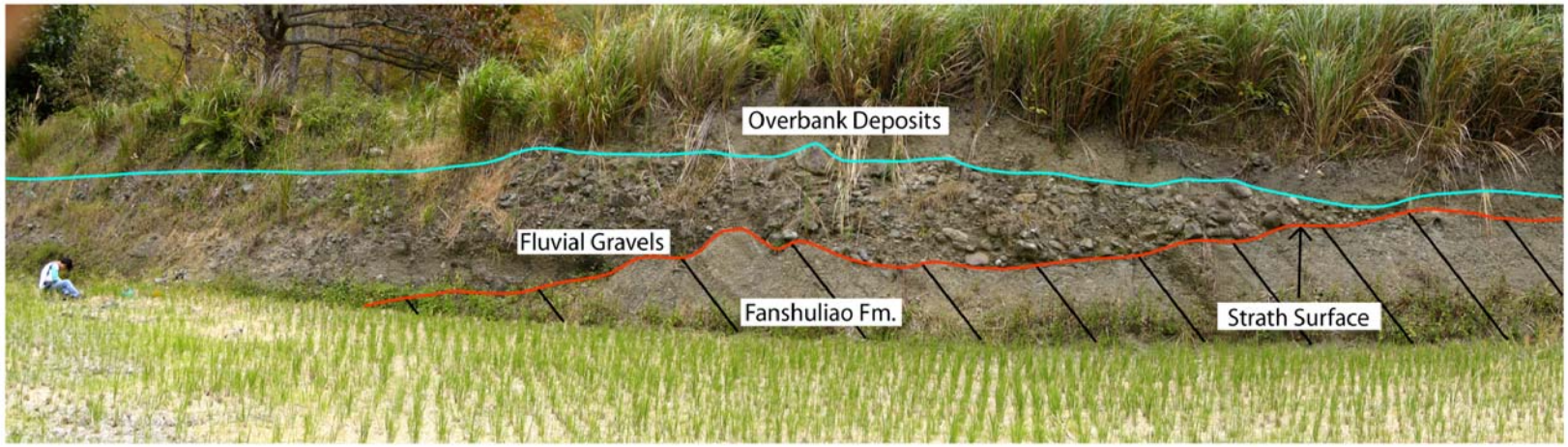

Figure 9. Natural strath exposure at QtI (site 17). The Bieh River is located behind the photographer to the west. Coarse fluvial gravel deposits 1-2 m thick, rest atop the Fanshuliao formation.

to a depth of 2 m ± 20 cm, only two sample pits exposed bedrock, neither of which contained fragments of detrital charcoal.

CHAPTER IV

DISCUSSION

Evidence for Holocene Strath Terraces within the Bieh River Drainage

With limited depth-to-strath surface data for most of the Bieh River terraces, it is difficult to determine if the terraces formed by aggradation, incision, or a combination of processes. Here, an aggradational terrace will be defined as a fluvial terrace mantled with at least 10m of fluvially-derived alluvium. Evidence for an aggradational origin is limited to the presence of the anomalous Qa terraces near the Tuluanshan Ridge (Plate 2), and the lack of depth to strath data. The >10 m sediment thickness of the northern Qa surface (Plate 1) suggests that some aggradation occurred within the Bieh River drainage, and may have resulted in the formation of several terraces within the drainage. An aggradational period has been recorded for a number of small drainages on the eastern flanks of the Coastal Range (Hsieh *et al.*, 1994), east of Fuli, where fill terraces are common. This suggests that even in an actively uplifting environment, aggradation can still occur with favorable climatic conditions. The beginning of this aggradational period was dated to 5080 ± 50 cal. yr B.P., based on a detrital charcoal fragment located near the bedrock strath below 30 m of alluvial gravels. Bieh River trench-wall exposures of thirteen sample pits indicated that the depth to the strath surface is usually deeper than two meters and no deeper than the terrace's height above the channel. If the majority of Qt surfaces within the drainage are aggradational, it would imply that late Holocene climate was sufficiently wet to produce sediment at a rate faster than the Bieh River could transport it. In addition, because several of the terraces are late Holocene in age,

incision of those terraces occurred relatively recently to produce the multiple terrace flights present within the drainage.

Alternatively; the Bieh River terraces might represent a period of active incision that resulted in the formation of strath terraces. Evidence for such an interpretation include: (1) at the southeast Qt5 surface (Plate 2), a pit excavated for collecting detrital charcoal fragments exposed the Lichi Mélange strath surface at a depth of ~ 200 cm. The presence of a strath terrace in the lower reach of the Bieh River, between flights of other terraces, suggests other terraces nearby may also be strath surfaces; (2) present-day geodetic studies suggest uplift rates of up to 20 mm yr^{-1}. In this context, extended periods of aggradation would be unlikely, because over several millennia the river channel itself would become highly elevated with respect to the floor of the Longitudinal Valley; (3) the aggradational Qa terraces, if related to the aggradational period documented 15 km to the east (Hsieh *et al.*, 1994), would likely be much older than the majority of terraces within the Bieh River drainage. Assuming uplift rates of 11 mm yr^{-1} along the Bieh River, the majority of terraces would be younger than 1600 years, much younger than the 5000 cal. yr B.P. Coastal Range aggradational period. Therefore, it is probable that the majority of river terraces within the Bieh River drainage are the result of incision, not aggradation.

Late Holocene Incision Rates

The low relief of the Bieh River longitudinal profile and the weak lithologies composing the bedrock channel suggest that uplift of the Coast Range is nearly matched

by incision of the Bieh River active channel. Assuming incision rates are similar to uplift rates, a millennial-scale uplift rate can be determined from the strath terraces of the Bieh River. Millennial-scale uplift-rate determination of the Longitudinal Valley fault requires accurate individual strath terrace heights above the active channel and qualitative ages of each strath terrace surface where:

$$\text{uplift rate (mm yr}^{-1}\text{)} = \text{terrace elevation (mm)} / \text{terrace age (yr)} \quad (1)$$

Using Equation 1, the Qt6, Qt8, and Qt9 terraces yield incision rates of 12.1 ± 2.1, 8.9 ± 1.4, and 12.9 ± 2.5 mm yr^{-1}, respectively. Incision rates are calculated from 2σ calendric age ranges and an assumed 15% error in DEM and sampling elevation data. Based on three detrital charcoal samples, the average incision rate is 11.3 ± 3.6 mm yr^{-1} (Table 1). Calculation of river incision rates assumes that river sinuosity, climate-related discharge, and local base level (elevation of the Longitudinal Valley floor) have remained relatively stable throughout the late Holocene. Since the spatial distribution of late-Holocene terraces show no major channel migration, only minor changes in sinuosity have taken place within the time span of strath terrace formation. Regional base level for the Bieh River is controlled at the intersection of the Hsiukuluan River in the Longitudinal Valley, which lies 7 km north of the southern Longitudinal Valley drainage divide. Since the elevation of the Longitudinal Valley at Fuli is 215 m and the Longitudinal Valley fault at Fuli is likely several hundred thousand years old, long-term uplift/aggradation rates are probably quite low, possibly less than 1 mm yr^{-1}. If correct, the low aggradation rate has little influence on millennial scale uplift/incision rates of the Bieh River. The effects of climatic variation cannot be ruled out given that two

aggradational river terraces (Qa surfaces on Plate 2) are located within the elevation range of other inferred strath terraces in the drainage. Unfortunately, the age of the aggradational period is uncertain, perhaps related to the 5000 ka aggradational period documented on the eastern side of the coast range (Hsieh *et al.*, 1994).

Fragments of detrital charcoal were collected from alluvial sediments accumulated on top of the strath surfaces and likely represent maximum rates of incision at each site. At Qt8, the calendric age of 1365-1225 cal. yr B.P. suggests rates of incision 25% lower than incision rates associated with Qt6 and Qt9. The discrepancy between uplift rates is not well understood, but could be the result of recycled detrital charcoal collected from the Qt8 terrace tread. The lack of intact wood fibers within the Qt8 detrital charcoal sample support this interpretation.

Late Holocene Horizontal Shortening Rates

Where GPS plate convergence vectors are known, Equation 2 from Angelier *et al.* (2000) can be used to calculate the uplift rate (u), where x is the net horizontal displacement (horizontal shortening rate), α is the angle between the strike of the fault and the known GPS convergence vector, and ζ is the inferred fault dip angle at the surface.

$$\text{uplift rate } (u) = x \cos\alpha \tan \zeta \qquad (2)$$

Where the uplift rate (u) is known, horizontal shortening (x) can be determined by rearranging equation 2 to:

$$x = \frac{u}{\cos\alpha \tan\zeta} \qquad (3)$$

Here, oblique convergence of the Philippine Sea plate can be used to calculate the horizontal-shortening rate (equation 3). The Angelier *et al.*, (2000) equation incorporates the obliquity (α) of Philippine Sea Plate motion by including the angle between the GPS-derived shortening vector and the strike of the fault (Figure 10).

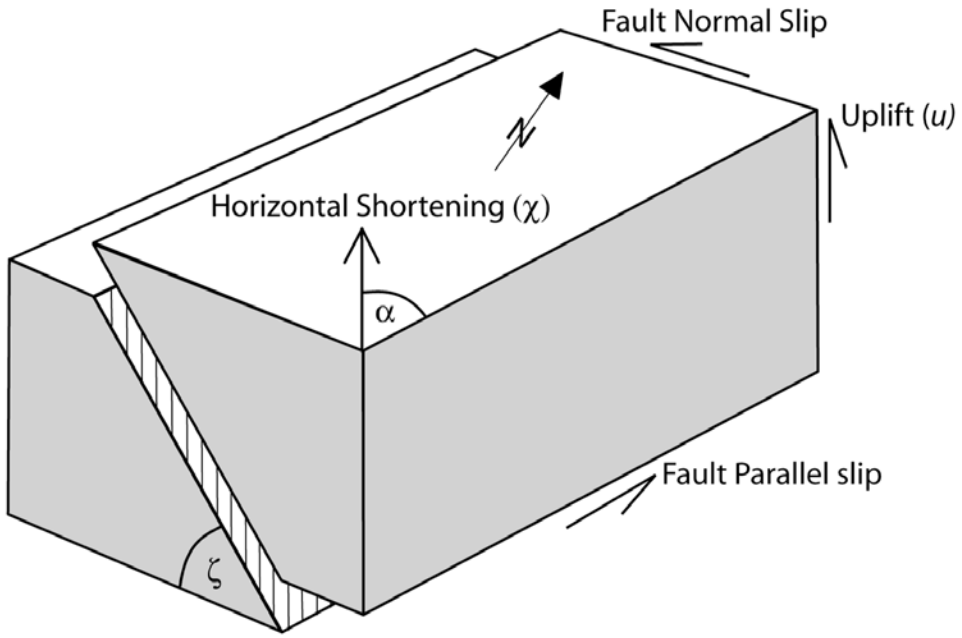

Figure 10. Block model for three-dimensional slip on the Longitudinal Valley fault. Horizontal shortening (χ) represents the maximum horizontal displacement vector incorporating fault parallel and fault normal motion on the Longitudinal Valley fault. Horizontal shortening is calculated using the uplift rate (*u*) obtained from the Bieh River strath terraces and the angle of obliquity (α), the angle measure between the horizontal shortening direction of the 326° and the strike of the fault (021°).

Assuming incision as a direct proxy for uplift, a 55° angle for α (the angle between the Longitudinal Valley fault strike of 021° and the GPS-derived relative displacement direction of 326° measured at Chihshang), and a 45° fault dip at the surface (measured from a Longitudinal Valley fault outcrop near Fuli), the horizontal shortening rates for Qt6, Qt8, and Qt9 are 21.1 ± 5.8, 15.5 ± 4.2, and 22.5 ± 6.3 mm yr^{-1},

respectively (Table 1). Errors associated with horizontal shortening rates were calculated using a 3° variability in the horizontal shortening vector, a ± 5° fault dip angle, and propagation of error from the original uplift rate calculations (Table 1). Averaging the three horizontal shortening rates yields a 19.7 ± 9.5 mm yr^{-1} shortening rate at 326°.

Comparison of Present-Day and Millennial-Scale Horizontal Shortening Rates

The millennial-scale geologic slip rate across the Chihshang segment is the product of interseismic creep, coseismic rupture, and postseismic creep. Since most studies have documented slip associated with aseismic creep, millennial-scale slip rates on the Chihshang segment will reflect the addition of coseismic rupture and postseismic creep to the 22 mm yr^{-1} near-field and 31 mm yr^{-1} far-field horizontal shortening rates, and the 13–21 mm yr^{-1} uplift rate (Table 2). Uplift rates calculated from terrace treads suggest an average horizontal shortening rate of 19.7 ± 9.5 mm yr^{-1}, only slightly lower than the 22 mm yr^{-1} rate determined by conventional geodesy at Chihshang (Lee and Angelier, 1993; Angelier *et al.*, 1997). However, the only conventional geodetic study (leveling) that captures deformation of the Bieh River gives an uplift rate of 21 mm yr^{-1} (Yu and Liu, 1989) that corresponds to a 37 mm yr^{-1} horizontal shortening rate, using Equation 3. Because Bieh River terraces sampled for detrital charcoal were located 3 to 3.5 km from the Longitudinal Valley fault and outside of the narrow Longitudinal Valley fault deformation zone, the 19.7 ± 9.5 mm yr^{-1} geomorphic horizontal shortening rate can be compared to GPS geodetic rates, typically on the order of 31 mm yr^{-1} (Table 2). Although the 19.7 ± 9.5 mm yr^{-1} geomorphic horizontal shortening rate is within error of the 31 mm yr^{-1} GPS-based rate (Yu *et al.*, 1997) and the 22 mm yr^{-1} conventional

Table 2
Calculated Uplift, Horizontal Shortening, and Strike-Slip Rates of the Longitudinal Valley Fault

Region and Measurement method	Slip rate measurement	Horizontal shortening rate (mm yr^{-1})	Uplift rate (mm yr^{-1})	Sinistral slip rate (mm yr^{-1})	Reference
Rueisuei					
paleoseismology	geologic	10.6	—	—	Fengler *et al.* (in prep)
paleoseismology	geologic	21.6-27.7	12.5-16.0	—	Chen *et al.* (in prep)
river incision	geologic	27.7	—	—	Shyu *et al.* (2006)
GPS	far-field plate motion	24.6-29.4	15.1-19.3	—	Yu and Kuo (2001)
InSAR	surface creep	0-5 (dip-slip)	—	—	Hsu and Bürgmann (2006)
Yuli					
GPS	far-field plate motion	35	—	—	Yu (1986)
GPS	far-field plate motion	18.7	—	—	Yu *et al.* (1997)
GPS and leveling	far-field plate motion	20.8-27.7	24.4	—	Yu and Kuo (2001)
geodetic network	surface creep	33	—	—	Yu *et al.* (1990)
InSAR	surface creep	32.7 (dip-slip)	—	—	Hsu and Bürgmann (2006)
Chihshang					
near-fault geodetic network	surface creep	22	—	—	Angelier *et al.* (1997)
near-fault geodetic network	surface creep	21	—	—	Lee and Angelier (1993)
near-fault geodetic network	surface creep	21	13	18	Angelier *et al.* (2000)
InSAR (Fuli)	surface creep	35 (dip-slip)	13	14	Hsu and Bürgmann (2006)
InSAR	surface creep	24 (dip-slip)	—	—	Hsu and Bürgmann (2006)
creepmeter	surface creep	17.3 and 19.4	—	—	Lee *et al.* (2001)
creepmeter	surface creep	15 and 16.2	—	—	Lee *et al.* (2003)
leveling (Fuli)	surface creep	—	21	—	Yu and Liu (1989)
GPS	far-field plate motion	31	—	—	Yu *et al.* (1997)
GPS	far-field plate motion	29.2-32.7	30	—	Yu and Kuo (2001)
river incision	geologic	19.7	11.3	—	This Study

geodetic rate measured at Chihshang (Lee and Angelier, 1993; Angelier *et al.*, 1997), it is on the lower end of most horizontal shortening and uplift measurements made on the Chihshang segment of the Longitudinal Valley fault (Table 2).

There are several possibilities why the millennial-scale geologic slip rates inferred from incision of the Bieh River are lower than regional GPS-based and local leveling-based rates suggest. First, radiocarbon-based ages of detrital charcoal fragments under estimate incision rates on terraces Qt6, Qt8, and Qt9. Detrital charcoal fragments from Qt8 and Qt9 were located within coarse alluvium an unknown height above the buried strath surface. Since both charcoal fragments come from alluvium above the strath surface, it is difficult to estimate the time between formation of the strath surface and deposition of coarse alluvium. The detrital charcoal fragment from Qt6 is located within overbank sediments that were deposited after terrace formation. Similarly, since the time between strath formation and deposition of overbank sediments on top of the strath surface is not constrained, the incision rate at Qt6 is likely lower than the 12.1 ± 0.7 mm yr^{-1} incision rate (Table 1). Recycled detrital charcoal fragments yielding ages older than their associated strath surface are unlikely for Qt 6 and Qt9, since both detrital charcoal fragments consisted of intact fibers, a good indicator for *in-situ* preservation. Excepting the reworked detrital charcoal results from the Qt8 surface, errors associated with radiocarbon sampling yield younger strath ages that result in high incision rates.

Second, late-Holocene vertical river incision has been outpaced by uplift of the Coastal Range. Considering the current relief of the Bieh River and relatively weak local lithologies, an incision deficit is unlikely. As noted by Burbank and Anderson (2001),

deficits in river incision with respect to high rates of uplift will yield unusually high-relief longitudinal profiles. Assuming a minor incision deficit of 3 mm/yr for the last 50 ka along the Bieh River, 150 m of relief will have been created within a short distance upstream of the Chihshang fault, resulting in very steep gradients within the lower Bieh River active channel. The Bieh River longitudinal profile shows no major break in slope or knickpoint near the active trace of the Chihshang segment and no regions of very steep gradient, aside from the steep gradient along the Tuluanshan section of the river (Figure 7). The gradient variation in the Tuluanshan section is likely due to the presence of less resistant lithologies upstream and downstream of this section.

From the Longitudinal Valley fault upstream to the Tuluanshan Formation (Plate 1), relatively weak lithologies prevail. Rocks of the Fanshuliao and Lichi formations are poorly indurated and erode easily, in particular the Lichi Mélange (Figure 4). The erosive ability of the Bieh River is highlighted by Fuli and Chihshang rain gauge data from 1998 to 2006 (Taiwan Central Weather Bureau, 2007). Rain gauge data show average annual precipitation of more than 200 cm yr^{-1}, punctuated by tropical cyclone-derived precipitation often exceeding 300 mm or more in a single day (Taiwan Central Weather Bureau, 2007). Central Weather Bureau data stations are located along the eastern the margin of the Longitudinal Valley (the lee side of the Coastal Range) and probably represent minimum rainfall for the Bieh River drainage as a result of orographic precipitation effects of the Coastal Range. The extreme precipitation events, often occurring multiple times per year, have the capacity to mobilize boulders greater than 1 m in diameter. Studies in the Central Range by Hartshorn *et al.* (2002) suggest the

majority of river incision occurs in Taiwan during floods produced by large rain events such as tropical cyclones. Testament to the erosive power of local streams, an 8 m high reverse fault scarp created during the September, 1999 Chi-Chi earthquake has been reduced to a small riffle 8 years after the event, highlighting the dynamic nature of Taiwan's river systems. Given the poorly indurated and highly sheared nature of the Lichi Mélange, it seems unlikely that the frequent high-discharge events the Bieh River experiences are insufficient to maintain equilibrium between uplift and incision.

Third, differential uplift and bedrock incision may have resulted in under estimation of river incision rates. For example, if only terraces within slowly uplifting regions are sampled, the resulting incision rates will be correspondingly low. Relative motion across the Yungfong and Tuluanshan faults, as well as deformation within the Lichi Mélange could lead to differential uplift and bedrock incision along the lower reach of the Bieh River. Since no age data for terraces downstream or upstream of the Yungfong fault exist, the longitudinal profile was used as a proxy for differential uplift. Because the Bieh River longitudinal profile (Figure 7) is a proxy for tectonic deformation, there are two convex regions that suggest variable rock uplift rates and or lithology. One convexity along the Bieh River occurs within the resistant Tuluanshan formation. Typically, more resistant lithologies located within regions of softer lithologies often yield lower concavities, and often times convexities (VanLaningham *et al.*, 2006). In contrast, the lower reach of the Bieh River downstream from the initial crossing of the Yungfong fault does not show the concavity expected from a region characterized by evenly distributed uplift (Figure 7). Downstream from the lower crossing of the

Yungfong fault, river slope decreases and a minor convexity is formed, suggesting possible motion on the Yungfong fault and differential uplift within the Lichi Mélange block.

If evenly distributed uplift and weak lithologies create strong longitudinal profile concavities, why is there a convexity along the lower reach of the Bieh River? One explanation is that differential uplift of the Lichi Mélange occurs at a higher rate than surrounding rocks along the Bieh River. Studies by Shyu *et al.* (2006) along the Hsiukuluan River, which drains the central Longitudinal Valley (Figure 2), show river incision rates apparently decreasing with increasing eastward distance from the surface trace of the Longitudinal Valley fault. Here, the decreased river incision rate is likely the result of a fault-bend fold, as the dip of the Longitudinal Valley fault increases at depth. A fault-bend fold model was not applied in the Bieh River drainage due to the chaotic nature of the Lichi formation.

Although unmapped, it is likely that small-scale northeast-trending faults accommodating horizontal shortening exist, obscured within the densely vegetated margins of the surface trace of the Longitudinal Valley fault. If true, horizontal shortening rates should decrease near the Longitudinal Valley fault as slip is partitioned along minor faults. Differential uplift of the lower reach of the Bieh River, downstream of the Yungfong fault, should produce tilted and uneven terraces. Unfortunately, there are no continuous terrace treads located along the entire lower reach of the river and most surfaces have been modified for farming and housing. Terrace correlation with pedogenic analysis is not possible in the Bieh River drainage due to the young age of

terraces and highly variable nature of sedimentation. Slopes of terrace treads in the reach downstream of the Yungfong show little or no variation with respect to the active channel (Figure 7). Given the lack of terrace tilting, it is likely that if regional differential deformation is occurring, it probably does not constitute a substantial portion of the total deformation of the drainage.

Finally, it is possible that the horizontal shortening rates obtained from the Bieh River strath terraces accurately reflect uplift and horizontal shortening over the last 1400 years and that millennial-scale horizontal shortening could be lower than the present-day geodetic rate. There is evidence of decadal-scale variation of uplift 10 km south of the Bieh River near Chihshang. According to local records (Angelier *et al.*, 2000), after the November 1951 earthquake, a sag pond formed rapidly on the footwall of the Chihshang segment east of Chihshang. As of 1989, subsidence was still occurring at a rate of ~ 1 mm yr^{-1} (Liu and Yu, 1989). If local variations occur on a decadal scale, then certainly millennial-scale variation is a possibility.

Secondary Faulting Within the Bieh River Drainage

Two secondary faults, the Yungfong and Tuluanshan, are exposed east of the Longitudinal Valley fault within the Bieh River drainage (Plate 1). It is uncertain whether these secondary faults are active faults. Here, evidence for fault activity is limited to geomorphologic indicators, primarily terrace distribution and the longitudinal profile. For example, the upstream river crossing of the Yungfong fault (the Lichi/Fanshuliao contact) is marked by a 90° northward bend (Plate 1). Here, the Bieh River flows roughly along strike for about 2.5 km, where soft rocks of the Lichi

formation appear to impede westward flow of the river, although they are less cohesive and poorly indurated with respect to the upstream Fanshuliao mudstone and sandstone. Given the lithologic variation between the Lichi and Fanshuliao formations, a knickpoint should be expected between the formations, assuming uniform uplift with no relative displacement along the Yungfong fault. At the upstream Yungfong contact (Figure 7), the river clearly crosses from Fanshuliao to Lichi Mélange, with no knickpoint present. There is a small slope perturbation at the downstream crossing, where the fault location is inferred but not directly located. The 90° northward deflection of the Bieh River at the Yungfong fault might be the result of initial blockage of the channel by a preexisting paleo-high, displacement along the Yungfong backthrust, or preferential erosion of the shear zone along the Yungfong fault.

In the case of the Tuluanshan fault, other than the existence of a clear knickpoint likely due to lithologic variation within the bedrock channel, there is no evidence suggesting Holocene activity. There are no linear geomorphic features at the base of Tuluanshan ridge to suggest otherwise. In addition, earthquake relocations from Kuochen *et al.* (2004) and Lee *et al.* (2006) show no evidence of an active east-dipping fault plane east of the main Longitudinal Valley fault suture.

Implications for Collisional Tectonics at Fuli

Based on three detrital charcoal fragments from Qt6, Qt8, and Qt9 that yield ages of 1395-555 cal. yr B.P., the average uplift rate of the Yungfong reach of the Bieh River is 11.3 ± 3.6 mm yr^{-1}. The relatively rapid uplift rate suggests that the Longitudinal Valley fault at Fuli must be a comparatively young structure. Based on the maximum

Coastal Range elevation of 1600 m near Fuli and an erosion rate of 5-8 mm/yr (Willet *et al.* 2003; Fuller *et al.* 2003) determined for the nearby eastern flanks of the Central Range, the age of the Coastal Range orogen at Fuli (set at the time of current sea-level emergence) is between 254 and 472 ka. The suture zone age at Fuli can also be estimated using the southward propagation velocity of the suture zone, assuming the modern-day emergent Coastal Range near Taitung is an analog to the Coastal Range at Fuli. Using Suppe's (1984) southward propagation velocity of 94 mm yr^{-1} and the 42 km distance between Fuli and the present-day emerging Coastal Range, the Fuli region of the Coastal Range emerged from present-day sea level around 450 ka ago. As a rough estimate, this method yields a result within the upper bound of the previous uplift estimation. The propagation calculation assumes that southward propagation of the fault zone occurs linearly, as does coastal range exhumation.

CHAPTER V

CONCLUSIONS

Results from three detrital charcoal fragments from terrace treads in the Bieh River drainage yield an average uplift rate of 11.3 mm yr^{-1}, suggesting the Coastal Range orogen at Fuli is a relatively young structure, likely younger than 500 ka. Incision rates from the Bieh River indicate a 19.7 ± 9.5 mm yr^{-1} average horizontal-shortening rate over the last 1395 cal. yr B.P. This horizontal-shortening rate is similar to near-field conventional geodetic measurements in the Fuli/Chihshang region. However, when compared to GPS-based rates, the average Bieh River horizontal-shortening rate is lower than GPS-derived horizontal-shortening rates, but within error of the GPS based horizontal shortening rates. Assuming the geomorphic data represent the regional millennial-scale uplift rate of the Bieh River, it is possible that current regional geodetic measurements may not reflect millennial-scale vertical and horizontal motion along the Longitudinal Valley fault.

The longitudinal profile and orientation of the Bieh River terraces suggests differential uplift may be occurring within the region of the Lichi Mélange and along the Yungfong fault, but may not produce observable variance in terrace slope with respect to the active channel. If differential uplift is presently occurring in the Bieh River drainage, it may explain differences between geologic and geodetic rates. Detailed geodetic studies and longitudinal profile modeling will help to constrain current uplift and horizontal shortening characteristics of the Bieh River drainage.

REFERENCES

Angelier, J., H. T. Chu, and J. C. Lee, (1997). Shear concentration in a collision zone: kinematics of the Chihshang Fault as revealed by outcrop-scale quantification of active faulting, Longitudinal Valley, eastern Taiwan. *Tectonophysics* **274,** 117–143.

Angelier, J., H. T. Chu, J. C. Lee, and J.C. Hu (2000). Active faulting and earthquake hazard: The case study of the Chihshang Fault, Taiwan. *Jour. Geodynamics* **29,** 151–185.

Barrier, E., and J. Angelier (1986). Active collision in eastern Taiwan: The Coastal Range. *Tectonophysics* **125,** 39–72.

Bonilla, M. G. (1975). A review of recently active faults in Taiwan, *U.S. Geol. Surv. Open-File Rep.* **75–11.**

Bonilla, M.G. (1977). Summary of Quaternary faulting and elevation changes in Taiwan. *Mem. Geol. Soc. China* **2,** 43–56.

Bonilla, M. G. (1999). A note on historic and quaternary faults in western Taiwan, *U.S. Geol. Surv. Open-File Rept.* **99-447**, 5 pp.

Burbank, D. W., and R. S. Anderson (2001). *Tectonic Geomorphology*, Blackwell Science, Malden, MA.

Chang, L. S. (1967). A biostratigraphic study of the Tertiary in the Coastal Range, eastern Taiwan, based on smaller foraminifera, *Proc. Geol. Soc. China* **10,** 64–76.

Chang, C.-P., J. Angelier, C. Y. Huang, and C. S. Liu (2001). Structural evolution and significance of a mélange in a collision belt: the Lichi Mélange and the Taiwan arc-continent collision. *Geol. Mag.* **138,** 633–651.

Chen, H. W., Academia Sinica, Taipei Taiwan, published on the Queensland University Advanced Center for Earthquake Studies website, http://www.quakes.uq.edu.au/Seminar/HChen.html, (last accessed June 2007).

Chen, W. S. (1988). Tectonic evolution of sedimentary basins in the Coastal Range, eastern Taiwan, *Unpublished Thesis*, Dept. of Geological Sciences, National Taiwan University, Taipei, Taiwan, 304pp.

Chen, W. S., and Y. Wang (1988). Development of deep-sea fan systems in Coastal Range basin, eastern Taiwan, *Acta Geol. Taiw.* **26,** 37–56.

Cheng, K. C. (1960). Report on the 1951 earthquake in Taiwan: *Proc. World Conf. Earthq. Eng*. **1,** 397–408.

Chi, W. R., J. Namson, and J. Suppe (1981). Record of plate interactions in the Coastal Range, eastern Taiwan, *Mem. Geol. Soc. China* **4,** 155–194.

Ching, K. E., R. J. Rau, and Y. Zeng (2004). Coseismic source model of the 2003 Chen-Kung, Taiwan, earthquake based on the GPS displacement observations, Presented at the Annual Meeting, Geophysical Society, Taoyuan, Taiwan.

Chung, L. H. (2003). Surface rupture reevaluation of the 1951 earthquake sequence in the middle Longitudinal Valley and neotectonic implications, *MS thesis*, National Taiwan University, Taipei, Taiwan, 138pp., (in Chinese with English abstract).

Fuller, C. W., S. D. Willet, N. Hovius, and R. Slingerland (2003). Erosion rates for Taiwan mountain basins: New determinations from suspended sediment records and a stochastic model of their temporal variation, *J. Geol.* **111,** 71–87.

Hartshorn, K., N. Hovius, W. B. Dade, and R. L. Slingerland (2002). Climate-driven bedrock incision in an active mountain belt, *Science* **297,** 2036–2038.

Hsieh, M. L., T. H. Lai, and P. M. Liew (1994). Holocene climatic river terraces in an active tectonic-uplifting area, middle part of the Coastal Range, eastern Taiwan, *J. Geol. Soc. China* **37,** 97–114.

Hsu, L. and Bürgmann, R. (2006). Surface creep along the Longitudinal Valley Fault, Taiwan from InSAR measurements, *Geophys. Res. Lett.* **33,** no. L0, 6312, doi:10.1029/2005GL024624.

Hsu, M. T. (1971). Seismicity of Taiwan and some related problems, *Bull. Intern. Inst. Seismol. and Earthq. Eng*. **8**, 41–160.

Hsu, T. L. (1955). The earthquakes of Taiwan, *Bank of Taiwan Quat. J.* **7**, 148–164.

Hsu, T. L. (1962). Recent faulting in the Longitudinal Valley of eastern Taiwan, *Mem. Geol. Soc. China* **1**, 95–102.

Hsu, T. L. (1976). The Lichi Mélange in the Coastal Range framework, *Bull. Geol. Surv. of Taiwan* **8**, 87–95.

Huang, T. Y. (1969). Some planktonic foraminifera from a bore at Shihshan, near Taitung, Taiwan, *Proc. Geol. Soc. China* **12,** 103–119.

Kirby, E. and K. X. Whipple (2001). Quantifying differential rock-uplift rates via stream profile analysis, *Geol.* **29**, 415–418.

Kuochen, H., Y. M. Wu, C. H. Chang, J. C. Hu, and W. S. Chen (2004). Relocation of the eastern Taiwan earthquakes and its tectonic implications, *Terr. Atmos. Oceanic.* **15**, 647–666.

Lee, J. C, and J. Angelier (1993). Localisation des deformations actives et traitement des données géodésiques; l'exemple de la faille de la Vallée Longitudinale, Taiwan, *Bull. Soc. Geol. France* **164,** 533–570.

Lee, J. C., J. Angelier, H. T. Chu, J. C. Hu, and F. S. Jeng (2001).Continuous monitoring of an active fault in a plate suture zone: a creepmeter study of the Chihshang Fault, eastern Taiwan, *Tectonophysics* **333,** 219–240.

Lee, J. C., J. Angelier, H. T. Chu, J. C. Hu, F. S. Jeng, and R. J. Rau (2003). Active fault creep variations at Chihshang, Taiwan, revealed by creep meter monitoring, 1998-2001. *J. Geophys. Res.* **108,** no. B11, 2528, doi:10.1029/2003JB002394.

Lee, J. C., H. T. Chu, J. Angelier, J. C. Hu, H. Y. Chen, and S. B Yu (2006). Quantitative analysis of surface coseismic faulting and postseismic creep accompanying the 2003, M_w = 6.5, Chengkung earthquake in eastern Taiwan, *J. Geophys. Res.* **111,** no. B0, 2405, doi: 10.1029/2005JB003612.

Liao, Y. H., L. C. Hwang, C. C. Chang, Y. J. Hong, I. N. Lee, J. H. Huang, S. F. Lin, M. Shen, C. H. Lin, and Y. Y. Gau (2003). Building Collapse and Human Deaths Resulting from the Chi-Chi Earthquake in Taiwan, September 1999, *Arch. Env. Health* **58,** 572–578.

Liu, J. G., C. Y. Lan, and W. G. Ernst (1977). The East Taiwan Ophiolite, *Mining Research and Service Organization*, Taipei, Taiwan, special report no. **1, 212**.

Lundberg, N., D. L Reed, C. S. Liu, and J. Lieske (1997). Forearc-basin closure and arc accretion in the submarine suture zone south of Taiwan, *Tectonophysics* **274,** 5–23.

Merritts, D. J., K. R. Vincent, and E. Wohl (1994). Long river profiles, tectonism, and eustasy: A guide to interpreting fluvial terraces, *J. Geophys. Res.* **99,** no. B7, 14,031–14,050.

Pazzaglia, F. J., T. W. Garner, and D. J. Merritts (1998). Bedrock fluvial incision and longitudinal profile development over geologic time scales determined by fluvial terraces, in *Rivers Over Rock: Fluvial Processes in Bedrock Channels*, Geophys. Monogr. Ser., **107,** edited by T. J.Tinkler and E. E. Wohl, AGU, Washington, D. C., 207– 235.

Page, B. M., and J. Suppe (1981). The Pliocene Lichi Mélange of Taiwan: its plate tectonic and olistostromal origin, *Am. J. Science* **281,** 193–227.

Ramsey, C. B. (2005). OxCal Version 3.10.

Shyu, J. B. H., K. Sieh, Y. G. Chen, and C. S. Liu (2005a). Neotectonic architecture of Taiwan and its implications for future large earthquakes, *J. Geophys. Res.*, **110,** no. B0, 8402, doi:10.1029/2004JB003251.

Shyu, J. B. H., K. Sieh, and Y. G Chen (2005b).Tandem suturing and disarticulation of the Taiwan orogen revealed by its neotectonic elements, *Earth Planet. Sci. Lett.* **233,** 167–177.

Shyu, J. B. H., K. Sieh, J. P Avouac, W. S. Chen, and Y. G. Chen (2006). Millennial slip rate of the Longitudinal Valley fault from river terraces: Implications for convergence across the active suture of eastern Taiwan. *J. Geophys. Res* **111,** no. B0, 8403, doi:10.1029/2005JB003971.

Shyu, J. B. H., L. H. Chung, Y. G. Chen, J. C. Lee, and K. Sieh (2007). Re-evaluation of the surface ruptures of the November 1951 earthquake series in eastern Taiwan, and its neotectonic implications, *J. Asian Earth Sci.*, in press.

Stuiver, M. and H. A. Polach (1977). Discussion: Reporting of ^{14}C Data, *Radiocarbon* **19,** 355–363.

Suppe, J. (1981). Mechanics of mountain building and metamorphism in Taiwan. *Mem. Geol. Soc. China* **4,** 67–89.

Suppe, J. (1984). Kinematics of arc-continent collision, flipping of subduction, and back-arc spreading near Taiwan, *Mem. Geol. Soc. China* **6,** 21–33.

Taiwan Central Weather Bureau (2007). Unpublished rain gauge data from the Fuli and Chihshang areas, eastern Taiwan.

Teng, L. S., W. S. Chen, Y. Wang, S. R. Song, and H. J. Lo (1988). Toward a comprehensive stratigraphic system of the Coastal Range, eastern Taiwan, *Act. Geol. Taiw.* **26,** 19–35.

United States Central Intelligence Agency (2007). *World Factbook 2007*, www.cia.gov/library/publications/the-world-factbook/geos/tw.html.

VanLaningham, S., A. Meigs, and C. Goldfinger (2006). The effects of rock uplift and rock resistance on river morphology in a subduction zone forearc, Oregon, USA, *Earth Surf. Process. Landforms* **31,** 1257–1279.

Wang, Y., and W. S. Chen (1993). Geologic map of eastern Coastal Range, Central Geologic Survey, Ministry of Economic Affairs, Taipei, Taiwan.

Whipple, K. X. (2004). Bedrock rivers and the geomorphology of active orogens, *Annu. Rev. Earth Planet. Sci.* **32,** 151–185.

Willet, S. D., D. Fisher, C. Fuller, E. C. Yeh, and C. Y. Lu (2003). Erosion Rates and Orogenic Wedge Kinematics in Taiwan inferred from Fission Track Thermochronometry, *Geol.* **31,** 945–948.

Wu, Y. M., Y. G. Chen, C. H. Chang, L. H. Chung, T. L. Teng, F. T. Wu, and C. F. Wu (2006). Seismotectonic structure in a tectonic suture zone: With new constraints from 2006 M_w 6.1 Taitung earthquake, *Geophys. Res. Lett.* **33,** no. L2, 2305, doi:10.1029/2006GL027572.

Yu, S. B., and C. C. Liu, (1989). Fault creep on the central segment of the Longitudinal Valley Fault, eastern Taiwan, *Proc. Geol. Soc. China,* **32,** 209–231.

Yu, S. B., D. D. Jackson, G. K. Yu, and C. C. Liu (1990). Dislocation model for crustal deformation in the Longitudinal Valley area, eastern Taiwan, *Tectonophysics* **183,** 97–109.

Yu, S. B., H. Y. Chen, and L. C. Kuo (1997). Velocity field of GPS stations in the Taiwan area, *Tectonophysics* **274,** 41–59.

Yu, S. B., and L. C. Kuo (2001). Present-day crustal motion along the Longitudinal Valley Fault, eastern Taiwan. *Tectonophysics* **333,** 199–217.